SPACE SCIENCES LABORATORY

UCBSSL No. 520/74

"AETHER DRIFT" AND THE ISOTROPY OF THE UNIVERSE

Period of Performance
1 July, 1974 - 30 June, 1975

Amount
$79,513

Principal Investigator
Richard A. Muller

Co-Experimenters
Luis W. Alvarez
Andrew Buffington
Terry Mast
Charles Orth
George Smoot

17 May, 1974

UNIVERSITY OF CALIFORNIA, BERKELEY

The Regents of the University of California
Space Sciences Laboratory
and
Lawrence Berkeley Laboratory
Berkeley, California 94720

UNOFFICI
COPY

UCBSSL No. 520/74

PROPOSAL FOR AN EXPERIMENT ON AN AIRBORNE PLATFORM: A SEARCH FOR ANISOTROPIES IN THE PRIMORDIAL BLACK-BODY RADIATION.

"AETHER DRIFT" AND THE ISOTROPY OF THE UNIVERSE

Principal Investigator
Richard A. Muller
University of California Space Sciences Laboratory
and Lawrence Berkeley Laboratory

Co-Experimenters
Luis W. Alvarez
Andrew Buffington
Terry Mast
Charles Orth
George Smoot

Mailing Address:
Lawrence Berkeley Laboratory
Bldg. 50, Rm. 240
Berkeley, California 94720
Telephone: (415) 843-2740 X5235

Period of Performance
1 July 1974 - 30 June 1975

Amount
$79,513.

May 17, 1974

Richard A. Muller
Principal Investigator

Kinsey A. Anderson
Director
Space Sciences Laboratory

August B. Manza, Manager
Campus Research Office

"AETHER DRIFT" AND THE ISOTROPY OF THE UNIVERSE:

A proposed search for anisotropies in the primordial black body radiation

ABSTRACT:

We intend to detect and map the large-angular-scale anisotropies in the 3 °K primordial black-body radiation with a sensitivity of 2×10^{-4} °K, and an angular resolution of about 15°. We will be able to detect the motion of the earth with respect to the distant matter of the Universe. In addition we will probe the homogeneity and isotropy of the Universe (the "Cosmological Principle"). We plan to use a 33 GHz Dicke radiometer with a front end temperature of 300 °K, flown at airplane altitudes. The NASA-Ames Earth Survey Aircraft (U-2) is the best vehicle of the several considered. A few hours of observation should be sufficient to detect an anisotropy. Several flights spread out over a year will be necessary to understand the source of the anisotropy in detail.

TABLE OF CONTENTS

I. AN OVERVIEW OF THE EXPERIMENT

A. Introduction

The earth is bathed in an apparently universal 3 °K microwave radiation from space. Its existence is the strongest evidence we have in support of the Big Bang theory of the Universe, and its observed isotropy to one part in 10^3 is the strongest evidence we have in support of the Cosmological Principle (the speculation that the Universe is isotropic and homogeneous on a large scale). Anisotropies smaller than one part in 10^3 are expected, but never have been unambiguously observed. We here propose to detect and map these small anisotropies with a sensitivity of 2×10^{-4} °K, an order of magnitude better than that of previous experiments. The study of the anisotropies observable with this sensitivity will provide a unique probe of the nature of the Universe.

Anisotropies in the radiation can arise in several ways. According to Special Relativity, there can be only one frame of reference in which the microwave radiation is isotropic; according to the Big Bang theory of cosmology, that frame is the one which is at rest with respect to the distant matter of the Universe which emitted the radiation. Motion with respect to this special frame is called "Aether Drift". Aether drift would cause an anisotropy in the cosmic microwave radiation that would vary as $\cos\theta$, where θ is the angle between the direction of motion and the direction of observation. Aether drift arises from the revolution of the earth around the sun, the rotation of our solar system around the Milky Way Galaxy, and the motion of the Milky Way Galaxy within the local cluster of galaxies. The sum of these motions should produce an anisotropy large enough (10^{-3} °K) for us to detect easily, despite the fact that it has not been unambiguously observed before.

Another source of anisotropy is the rotation of the universe as a whole. Such rotation would yield a polar-equatorial anisotropy (with a component proportional to cos2θ) with a magnitude of 10^{-3} °K, even if the spin rate were so low that the Universe had only rotated through 10^{-4} of a complete revolution since the Big Bang. Other anisotropies could exis because of non-uniformities in the matter distribution of the Universe, or variations in the rate of the Hubble expansion with direction. Very general arguments based on the Big Bang model and causality lead one to expect inhomogeneities of this type ranging in size between 3° and 75°. (These same general arguments are used to explain the existence of the observed super-cluster of galaxies.) When we do detect an anisotropy, a study of its angular dependence will be the key to understanding its cau

Previous experimental searches for anisotropies have been limited poor experimental resolution and large backgrounds. A better experiment is now feasible due to recent developments in low-noise amplifiers at fr quencies above 30 GHz where the main background signal (synchrotron emis sion from our own galaxy) is less intense. Only within the last two yea have commercial low-noise amplifiers become available at these frequenci Even so, an experiment above 30 GHz requires operation at high altitudes in order to reduce signals from the anisotropies distribution of atmospheric water vapor and oxygen. In addition, the equipment must be carefully leveled to accuracies in the minute-of-arc range in order to avoi systematic errors from looking through different pathlengths of even a uniform atmosphere. Fortunately, NASA now has several airborne laboratories that could meet the requirements of this experiment. In particu the NASA-Ames Earth Survey Aircraft (U-2) would be an excellent platfor

B. Experiment Design

A single measurement of the intensity of the black-body radiation at any one frequency is sufficient to determine the characteristic temperature of that radiation. If the radiation is Doppler-shifted (by Aether drift, rotation of the Universe, etc.) the black-body nature of the frequency spectrum is unchanged, but the characteristic temperature is shifted. The ultimate goal of this experiment is a differential temperature map of the cosmic sphere in a frequency band where the cosmic black-body radiation dominates. Such an experiment is, in principle, considerably easier than the task of measuring the absolute temperature of the sky because we do not have to measure the magnitude of systematic contributions such as oxygen, but can simply arrange our equipment such that the effects cancel. Most of the cosmic black-body radiation signal will also cancel, of course, so that we will just be left with a measurement of the difference in signal from two parts of the sky. Fortunately, absolute measurements of temperature are not required; difference measurements are sufficient to search for Aether Drift, Spin of the Universe, proto-Supercluster inhomogeneities, and other features of great interest to cosmology. (See Section IIA for more discussion.)

We plan to use a twin-horn "Dicke Radiometer" similar in concept to those used by the previous experimenters in the field. Two nearly identical microwave antennas are pointed in opposite directions, but at the same zenith angle:

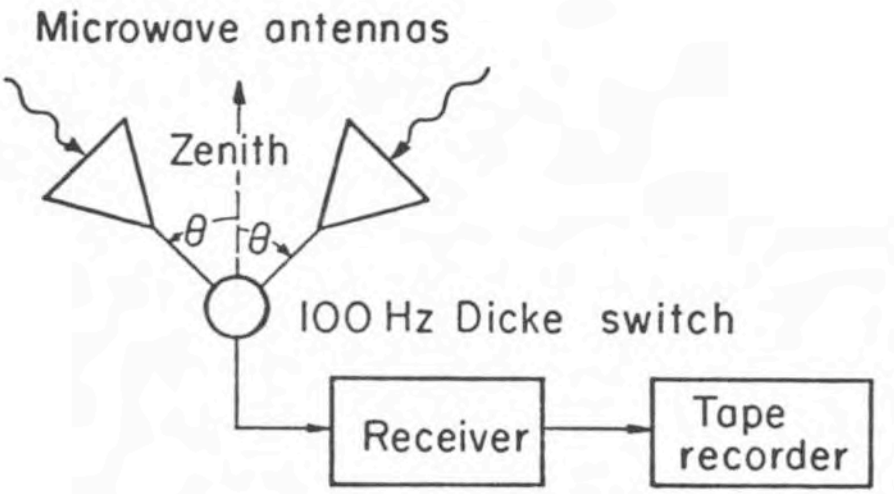

Figure 1. Two horn Dicke Radiometer. The low noise synchronous receiver detects signals at the switching frequency.

Although the antennas will have beam patterns approximately 5° wide, we plan to analyze our data in 15° bins. The experiment will detect any difference in signal greater than 2×10^{-4} °K received by the two antennas due to an anisotropy in the cosmic black-body radiation.

In order to cancel any spurious signal that may come from slight differences between the two antennas, they are physically interchanged at periodic intervals (once per minute). Spurious signals arising from statistical fluctuations in receiver noise are reduced by using a long integration time (two hours) for each resolution element in our map. Receiver drift is eliminated as a source of spurious signal by using a single receiver which is switched back and forth between the two antennas with a frequency rapid compared to drift frequencies; the receiver output is fed into a phase sensitive detector which looks for a signal synchronous with the switching.

C. Sources of Error

The sensitivity of past measurements has been limited by various combinations of detector noise, atmospheric emission, and galactic emission Thus, a detailed understanding and comparison of these contributions is crucial to the design of an experiment that plans to improve on the state of the art by an order of magnitude.

Galactic emission was a major source of systematic error for previous experiments. Below 1 GHz, galactic emission is more intense than the 3 °K cosmic black-body radiation. The intensity of this emission at frequency f (measured in degrees Kelvin) falls off roughly as f^{-n} where the spectral index n is approximately 2.7. This galactic emission is highly anisotropic, as the following map shows:

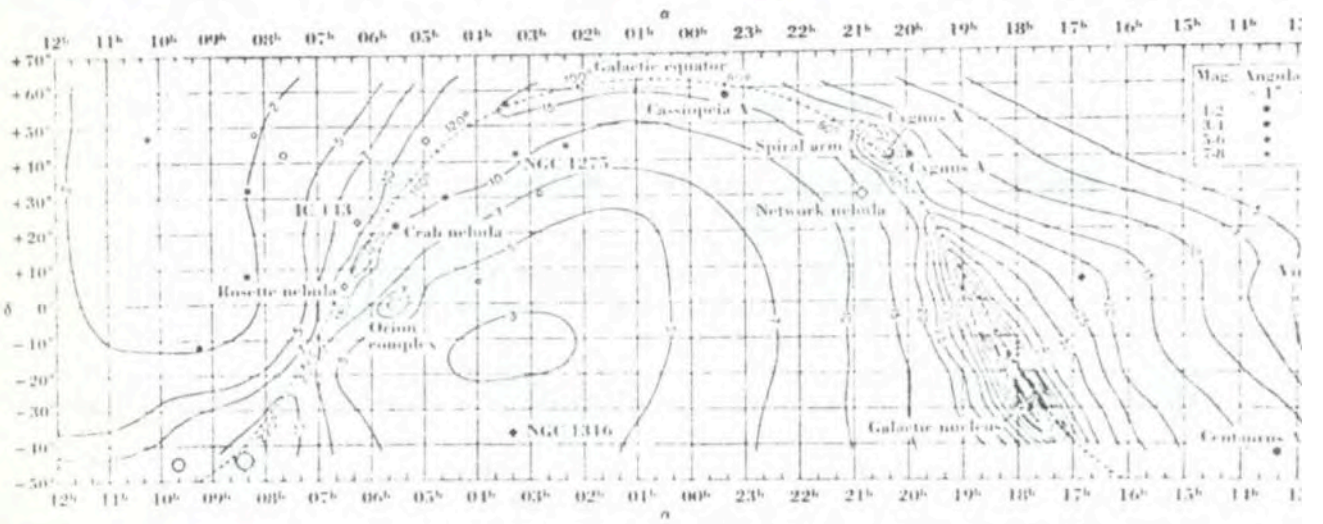

Figure 2a The radio sky at 0.25 GHz (from J. Kraus, Radio Astronomy, Mc-Graw Hill, 1966).
α is right ascension, δ is declination.

For comparison, we show the expected anisotropy for the Aether Drift, including galactic motion. The plots are at different frequencies, so only the shape of the features, and not the magnitudes, should be compared.

(See also Table I, page 18).

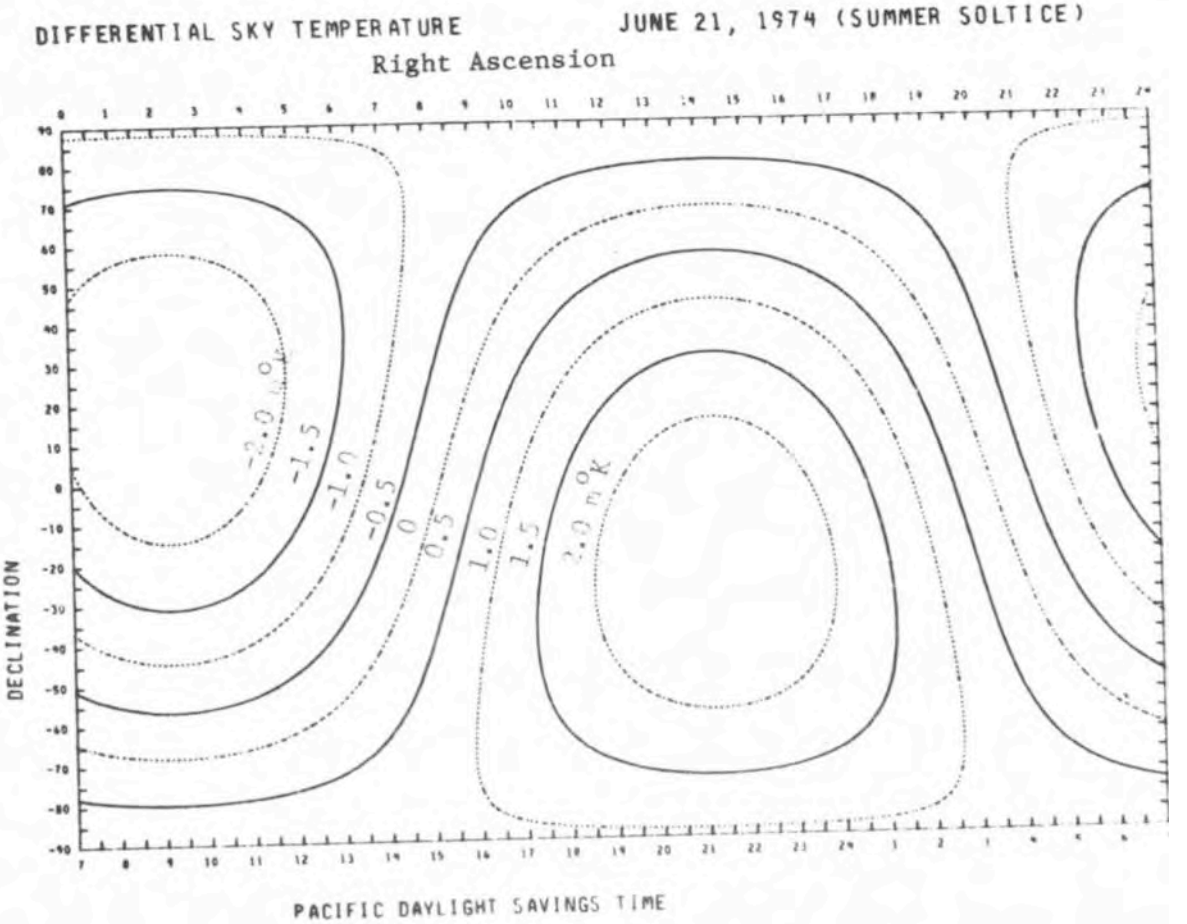

Figure 2b: Differential Sky Temperature resulting from a solar system velocity of 300 km/sec towards Virgo (14 hours, - 20°) combined with the velocity of the earth around the sun which for summer solstice is 30 km/sec towards Pisces (0 hours, 0°)

Above 1 GHz, the intensity of the black-body radiation dominates; however the galactic emission is still the major source of anisotropy. If the spectral index which governs the frequency behavior of the radiation were the same for all regions of the sky, one could reliably extrapolate the low frequency maps to higher frequency. In fact this very procedure was used in the most precise experiment to date: that by E.K. Conklin (Nature 222, 971, 1969). Unfortunately, the spectral index does vary between 2.4 and 2.9 for different regions of the sky, leading to a frequency depen-

dence in the map. This variation is not well mapped, so an accurate extrapolation is impossible. (Even if it were, the extrapolation would be limited by the accuracy to which the power law is followed.) In the figure on the next page we have plotted the galactic anisotropy (defined as the difference in power received in the two antennas, measured in degrees Kelvin) as a function of frequency. The three straight lines represent the range of spectral indices expected; the separation between the lines represents the uncertainity in the extrapolation. Also plotted are the expected signal due to Aether Drift: the upper curve for the motion of the Milky Way galaxy, and the lower one for the motion of the earth around the sun. In addition we have plotted Conklin's data point at 8 GHz; note that its magnitude (1.6×10^{-3} °K) is approximately equal to the uncertainty in the galactic map at that frequency.

To improve on Conklin's result, we must operate at higher frequencies where noise from the atmosphere becomes much more serious. In the figure on page 11, we have plotted the noise expected from atmospheric sources as a function of frequency. These sources are discussed in greater detail in section IIC; here we shall merely indicate the major features of the plot:

Non-uniform distribution of Water: Clouds of water vapor unevenly distributed over the antennas will give a signal. The plot corresponds to a 20% difference at 45,000 ft, where 2-3 μ precipitable water vapor are present. At 65,000 ft (the altitude of the U-2), the water vapor signal is negligible. At mountain-top altitudes, where much more water is present (1-2 mm), a much smaller difference (0.04%) would give the signal indicated on the plot; the expected anisotropies are much larger. Thus for

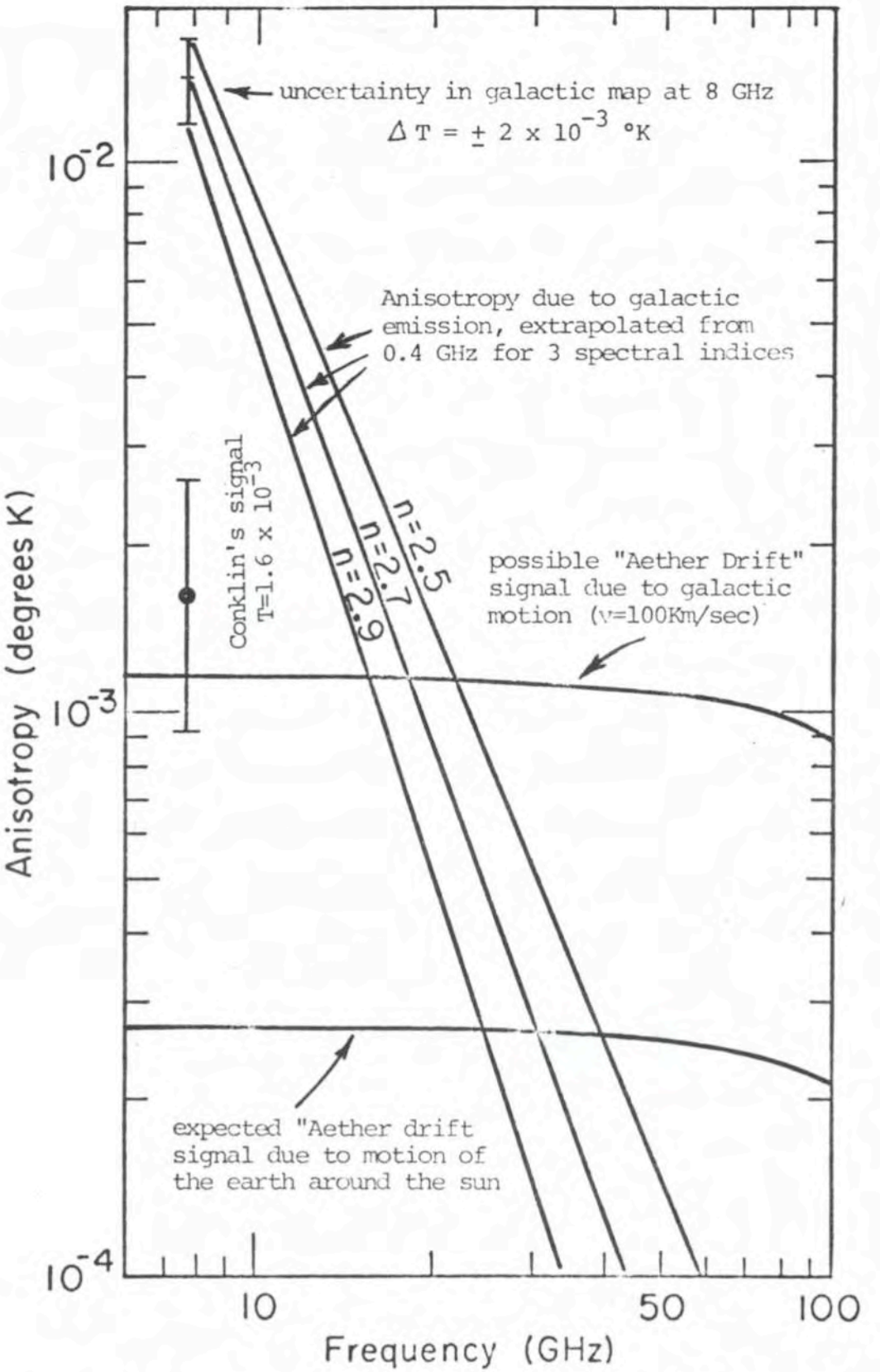

Figure 3: Expected anisotropies from 6 to 100 GHz. The "Aether Drift" signals decrease with increasing frequency because the plotted anisotropy is in

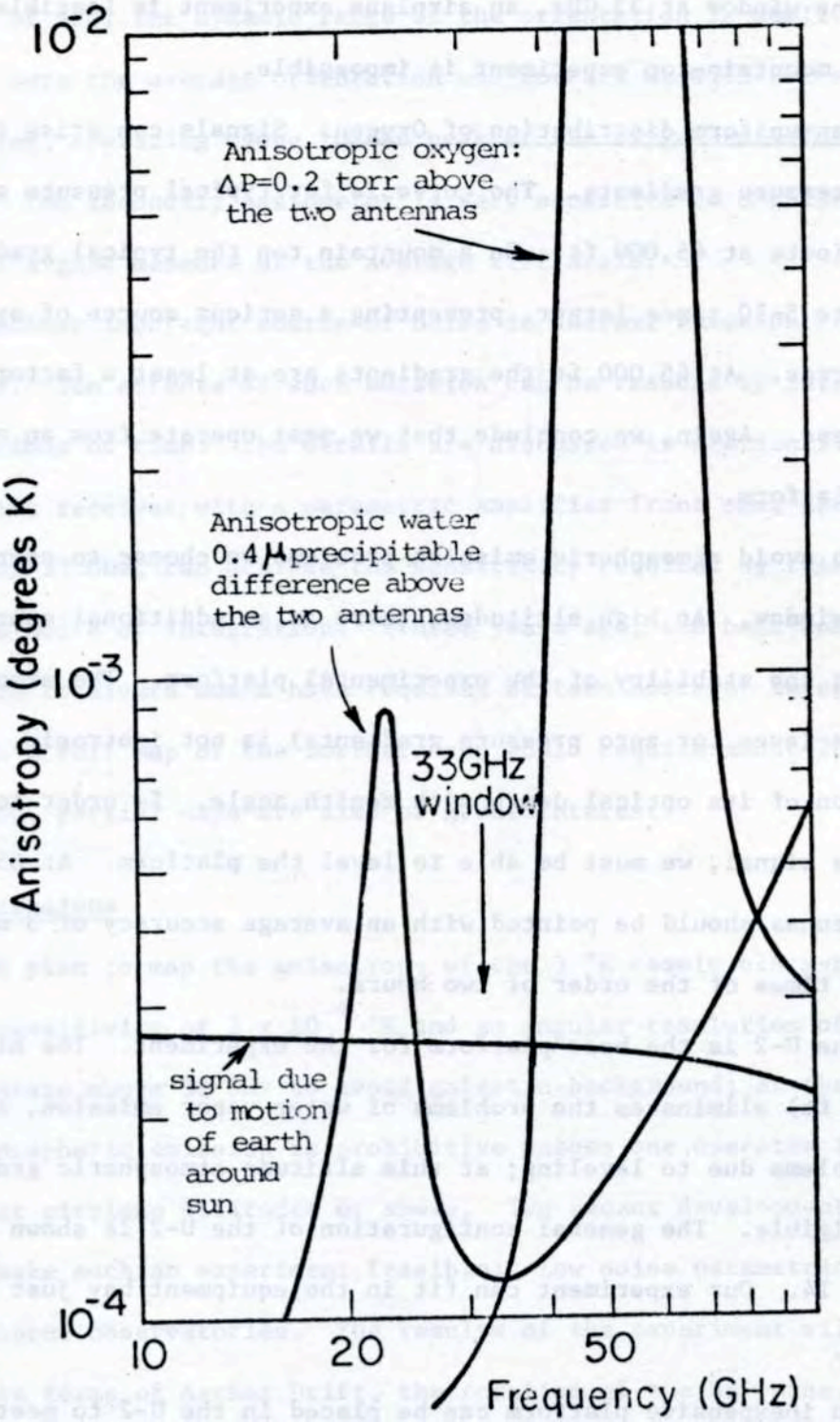

Figure 4: Anisotropic noise signals expected from water vapor and oxygen at 45,000 ft. At 65,000 ft (the proposed flight altitude), the amount of water vapor present is <<1 μ, and the oxygen anisotropy is reduced by a factor of 3.

the window at 33 GHz, an airplane experiment is feasible, and a mountain-top experiment is impossible.

Non-uniform distribution of Oxygen: Signals can arise from pressure gradients. The curve is for typical pressure gradients at 45,000 ft. On a mountain top the typical gradients are 5-10 times larger, presenting a serious source of systematic error. At 65,000 ft the gradients are at least a factor of 3 less. Again, we conclude that we must operate from an airborne platform.

To avoid atmospheric emission problems we choose to operate in the 33 GHz window. At high altitudes, there is an additional source of difficulty; the stability of the experimental platform. The atmospheric emission (even for zero pressure gradients) is not isotropic, due to the variation of its optical depth with zenith angle. In order to avoid a spurious signal, we must be able to level the platform. At 65,000 ft, the antennas should be pointed with an average accuracy of 3 minutes of arc for times of the order of two hours.

The U-2 is the best platform for the experiment. The high altitude (65,000 ft) eliminates the problems of water vapor emission, and minimizes the problems due to leveling; at this altitude atmospheric gradients will be negligible. The general configuration of the U-2 is shown in the figure on page 14. Our experiment can fit in the equipment bay just behind the cockpit.

An inexpensive platform can be placed in the U-2 to meet the orientation requirement. Our platform will not be required to take out the instantaneous oscillations of the U-2 about the vertical; it will merely orient the antennas so that they oscillate, on the average, about the vertical. Because of the exceptional stability of the U-2 (mean roll amplitude 10

minutes of arc) the dynamic range of the orientation is small. In order to make sure the average orientation was correct we will use a second radiometer, operating close to the peak of the oxygen emission line at 60 GHz. The secondary radiometer is very sensitive to angular tilt and provides a good measure of the average tilt angle.

Another important source of noise is thermal emission from within the receiver. The effects of such emission can be reduced by integrating for long periods of time: the details are discussed in section IIC. A state-of-the-art receiver with a parametric amplifier front end, operating in the window at 33 GHz, can achieve the sensitivity required by this experiment with two hours of integration. (Three years ago, the best commerically available receivers would have required sixteen hours of integration.) Although a full map of the northern sky would require about 200 hours of operation, partial maps are also of great interest.

D. Conclusions

We plan to map the anisotropy of the 3 °K cosmic black-body radiation with a sensitivity of 2×10^{-4} °K and an angular resolution of 15°. We must operate above 30 GHz to avoid galactic background; at these frequencies atmospheric emission is prohibitive unless one operates in the 33 GHz window at airplane altitudes or above. Two recent developments in technology make such an experiment feasible: low noise parametric amplifiers, and airborne observatories. The results of the experiment will be interpreted in terms of Aether Drift, the rotation of the Universe, and anisotropies related to the creation of super-clusters of galaxies.

GENERAL CONFIGURATION -MODEL U-2

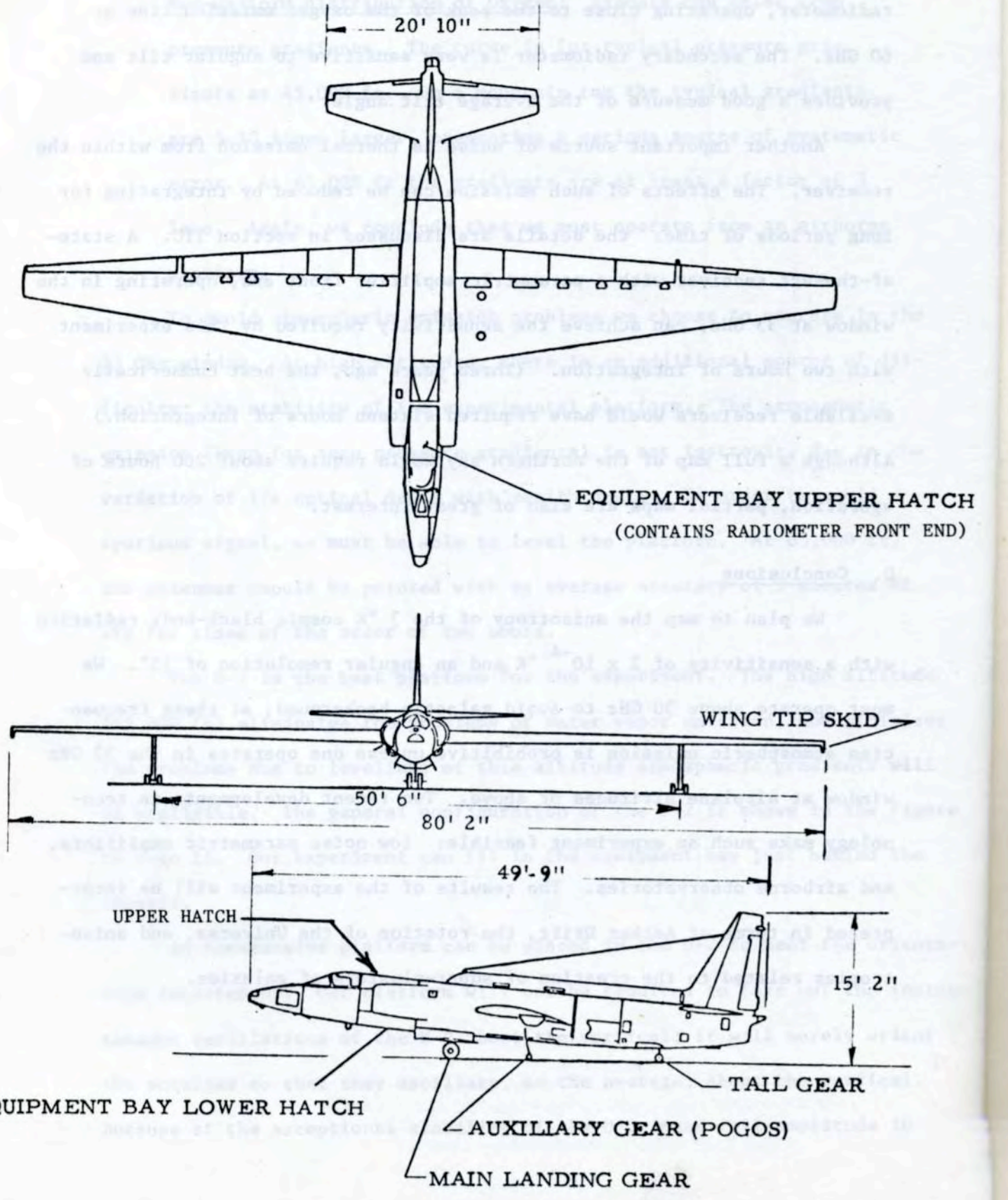

II. A DETAILED LOOK AT THE EXPERIMENT

A. Theory of the 3 °K radiation and expected anisotropies

In 1965, Penzias and Wilson found an unexpectedly large background in their 7 cm microwave receiver. Many workers have since confirmed the existence of this background, covering a range in wavelengths from several millimeters to many centimeters. The figure below shows the measurements, together with a 2.7 °K black-body Planck distribution. Also shown in the figure are intensities indirectly deduced from measurements of the absorption spectra of cyanogen molecules around nearby stars, covering short wavelengths absorbed by the earth's atmosphere. The best data in the millimeter region (Muehlner and Weiss, Phys. Rev. D, 7, 326 (1973)) marked with the letter M, clearly shows the expected turnover.

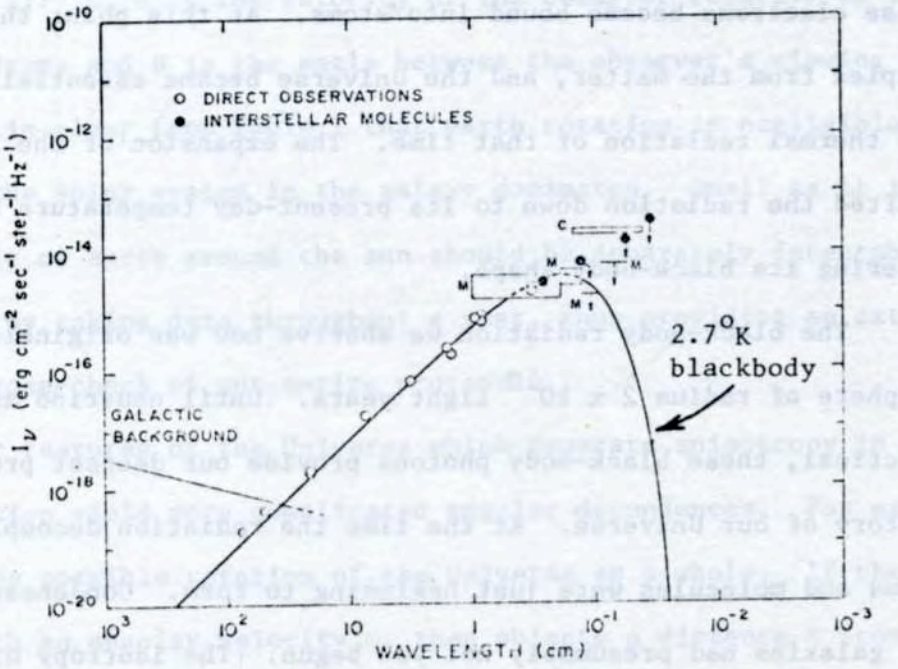

Figure 5: Measurements of the microwave background. (Taken from P. Thaddeus, Ann. Rev. Astron. and Astrophys. 10, 305 (1972))

The measurements are all consistent with a black-body shape for the radiation, although "grey-body" distributions with higher temperature cannot be ruled out until better measurements are achieved above the peak of the curve. A number of measurements have also been made of the directionality of this radiation: no significant departure from isotropy has ever been seen, down to an accuracy of about one tenth of a percent.

Most cosmologists take this radiation to be a relic from past epochs when our universe was much hotter and denser than it is now. Indeed, the presence of the black-body radiation provides the strongest evidence to date for such a "Big Bang" origin of the Universe. In these early epochs the high temperatures and densities kept almost all matter in an ionized state. Free electrons provided the thermal coupling between radiation and matter. When the expanding Universe had cooled to approximately 4000 °K, these electrons became bound into atoms. At this point the radiation decoupled from the matter, and the Universe became essentially transparent to the thermal radiation of that time. The expansion of the Universe then redshifted the radiation down to its present-day temperature of 2.7 °K without altering its black-body shape.

The black-body radiation we observe now was originally radiated from a sphere of radius 2×10^{10} light years. Until neutrino astronomy becomes practical, these black-body photons provide our deepest probe into the past history of our Universe. At the time the radiation decoupled from matter, atoms and molecules were just beginning to form. Condensation into stars and galaxies had presumably not yet begun. The isotropy of the black-body radiation is the strongest evidence that the early Universe was isotropic and homogeneous when viewed on a large-size scale (the "Cosmological Principle").

If in our measurement we observe an anisotropy of the black-body

radiation, the angular size of the anisotropy will suggest the mechanism which generated it. Motion of our earth reference frame relative to the "rest frame" defined billions of years ago by the last-scattering of the black-body photons is one mechanism that could produce an anisotropy. This modern "Aether Drift" experiment will show that vector sum of all the various motions of the earth listed in Table I. According to Special Relativity (Peebles and Wilkinson, Phys. Rev. 174, 2168 (1968)), motion of an observer relative to the uniform black-body radiation leaves the distribution shape of the radiation the same, but alters the observed black-body temperature to

$$T(\theta) = \frac{T_o\sqrt{1 - \beta^2}}{1 - \beta\cos\theta} \approx T_o\,(1 + \beta\cos\theta)$$

where T_o = 2.7 °K, β is the velocity of the observer relative to the black-body rest frame and θ is the angle between the observer's viewing direction and β. It is clear from Table I that earth rotation is negligible and that motion of the solar system in the galaxy dominates. Small as it is, the annual orbit of earth around the sun should be separately detectable by our experiment by taking data throughout a year, thus providing an extremely powerful cross-check of our entire procedure.

Other features of the Universe which generate anisotropy in the black body radiation yield more complicated angular dependences. For example, consider the possible rotation of the Universe as a whole. If the universe rotates with an angular velocity ω, then objects a distance R from us, and at an angle θ to the axis of rotation, will have a velocity $v_\theta = \omega R \sin\theta$, which, when added to its Hubble recessional velocity, yields a second order Doppler shift (due to time dilation) that depends on θ. The variation

TABLE I: MOTIONS OF THE EARTH RELATIVE TO "REST" FRAME

Source of Motion	Expected Velocity[(a)] (km/sec)	Anisotropy[(b)] (°K)
1. Earth Rotation	0.46	0.1×10^{-4}
2. Orbit around Sun	29.8	5.3×10^{-4}
3. Solar System in Galaxy	270 ± 40	$(49 \pm 7) \times 10^{-4}$
4. Galaxy around Local Cluster	80 ± 20	$(14 \pm 4) \times 10^{-4}$
5. Total Solar System around Local Cluster	315 ± 15	$(57 \pm 3) \times 10^{-4}$
6. Local Cluster relative to Black-Body	?	?

(a) Our source for velocities from 3-5 is D.W. Sciama, "Astrophysical Cosmology" pages 183-236, Proceedings of the International School of Physics Enrico Fermi, Course XLVII, Academic Press, New York, 1971.

(b) Calculated according to the formula $\Delta T = T_{max} - T_{min} = 2T_o\beta$ where β = velocity/velocity of light. This formula gives the peak-to-peak amplititude of the anisotropy for two horns separated by 60°.

should be axially symmetric, and its first order term (proportional to cos (2θ)) would be easily distinguishable from Aether Drift. A detailed analysis by Collins and Hawking (Monthly Notices of the Royal Astronomical Society 162, 307, (1973)) shows that if the Universe rotated at a rate of once per 10^{14} years, an anisotropy of 10×10^{-4} °K would result.

Detection of an overall rotation of the universe would be of great philosophical and cosmological importance. According to Mach's Principle, the existence of local inertial frames is caused by the mass of the distant galaxies, implying that the apparent rotation of the universe is zero. A discovery of non-zero rotation (which is allowed by General Relativity) would cast the entire Machian philosophy of matter and space-time into doubt.

Inhomogeneities in the matter distribution or in the expansion of the Universe should likewise lead to an anisotropy of the black body radiation. Although these might in principle give a cos (2θ) term which would be confused with spin, it is much more likely instead that they would yield higher order terms. Most cosmologists believe that an experiment an order of magnitude more sensitive than previous experiments is bound to detect such an inhomogeneity. Such inhomogeneities have been related, in certain theories, to the existence of the observed super-clusters of galaxies.

In some of these theories the Universe was initially completely inhomogeneous. The approximate homogeneity we now observe came about by the transport of energy and momentum that occurred early in the Big Bang. There are limits on the angular scale size of regions which could have been isotropized this way: a given region of space could not have received any homogenizing signal from further away than the distance light could travel between the time of the Big Bang and the time of the decoupling of radiation and matter.

Weinberg has calculated the angular size of isotropized regions in the sky which could have been generated this way ("Gravitation and Cosmology: Principles and Applications of the General Theory of Relativity", Wiley, New York, 1972, page 525. He reports that isotropy larger than just a few degree of angle in the sky requires a primordial homegeneity.* A good sky map, with the temperature of the black-body radiation measured with fractional millidegree temperature accuracy in 15° angular bins might in fact show such residual anisotropies, thereby disclosing information about the size of the density homogeneity in the early universe, even before matter and radiation were uncoupled.

Most other sources of anisotropy should result in an angular scale too small for us to observe with this experiment (planned resolution 15°), but might conceivably occur with a larger than expected scale. Such small-scale anisotropies could be due to inhomogeneities in the primordial plasma, or nascent galaxies, or they might be the first indication of discrete sources. Such emission anisotropies would appear as bright spots on the sky. Dark spots could also occur due to the absorption of some of the black-body radiation by large objects along the line of sight. A high density of energetic electrons in galactic clusters might attenuate the black-body radiation, by scattering it to higher frequencies. Such a cloud of electrons and their associated protons could help provide the mass needed for gravitational binding of galactic clusters.

The following table summarizes the possible causes of an inhomogeneity in the black-body radiation, and states the features of its angular distribution which would help distinguish it.

---

*For the case of an ionized intergalactic medium providing the mass to close the universe gravitationally this size grows to perhaps 1/10 of the sky, since the uncoupling of matter and radiation then took place at a much later time.

TABLE II: SOURCES OF ANISOTROPY AND THEIR ANGULAR DISTRIBUTIONS

Aether Drift - motion around sun	$\cos\theta$; amplitude varies (sinusoidally) during a year
Aether Drift - motion of galaxy	$\cos\theta$
Spin of Universe	$\cos(2\theta)$ although higher order terms possible
Primordial Inhomogeneities	$\cos(n\theta)$, n probably large
Other Inhomogeneities	correlated position in sky with suspected source

B. Previous techniques and measurements

The table below summarizes the large-angular-size isotropy measurements that have been reported. Both Conklin and Henry (references c & g) claim to see a small anisotropy in their data, but we feel both experiments suffer from poor statistical significance or from systematic difficulties in data interpretation.

TABLE III: SUMMARY OF MEASUREMENTS OF ANISOTROPIES OF LARGE ANGULAR SCALE IN THE MICROWAVE BACKGROUND

(The data used in reference e include those used in reference d.) All values of $\Delta T_\gamma / T_{\gamma o}$ bsed on an assumed value $T_{\gamma o} = 2.7$ °K.

(cm)	Type	$T_\gamma / T_{\gamma o}$ (%)	Reference
7.35	r.m.s.	10	a
7.35	r.m.s.	3.7	b
3.75	24 hours	0.06 ± 0.03	c
	12 hours	0.18 ± 0.08	
3.2	24 hours	0.03 ± 0.08	d
	12 hours	0.06 ± 0.06	
3.2	24 hours	0.04 ± 0.06	e
	12 hours	0.20 ± 0.24	
0.8	24 hours	0.28 ± 0.43	f
3.0	24 hours	.1 ± .03	g

---

[a]A.A. Penzias and R.W. Wilson, Ap. J., 142, 419, (1965).
[b]R.W. Wilson and A.A. Penzias, Science, 156, 1100, (1967).
[c]E.K. Conklin, Nature, 222, 971, (1969).
[d]R.B. Partridge and D.T. Wilkinson, Phys. Rev. Letters, 18, 557, (1967).
[e]D.T. Wilkinson and R.B. Partridge, quoted by R.B. Partridge, American Scientist, 57, 37 (1969).
[f]S.P. Boughn, D.M. Fram, and R.B. Partridge, Ap. J., 165, 439 (1971).
[g]P.S. Henry, Nature, 321, 516 (1971).

After Penzias and Wilson had completed the initial survey with their large microwave horn, groups from Princeton and Stanford carried out more

precise isotropy measurements using microwave horns arranged to cancel most of the sources of systematic error. Conklin's instrument employed two horns 60° apart between which the receiver was switched many times per second. In addition, the entire apparatus was rotated evey five minutes. In order to avoid the necessity of measuring and removing atmospheric contributions, Conklin performed his experiment atop White Mountain. The Partridge measurements used a zenith reference horn and a reflector system to direct the main horn beam. Daily atmospheric variations were averaged out by taking data throughout the year and analyzing the measurements in terms of sidereal time. Henry's apparatus employed two horns 90° apart, symmetrically placed about the vertical. The instrument was rotated every five minutes. A balloon flight to 24 km eliminated the need for atmospheric corrections, but the data-taking was limited to a single 12-hour flight.

Since the experiments of Conklin and Henry are the most sensitive, and since both have reported an anisotropy, we will examine their measurements in more detail. We also discuss an ongoing experiment by Weiss at the end of this section. Figure 6 shows Conklin's data, the results of 23 continuous days of running at White Mountain. Solar radiation was able to enter Conklin's system during daylight, thus no useable data were obtained between 10h and 18h (dotted gap). We have marked the location of the Milky Way disc for Conklin's latitude on the plot (arrows). The quantity plotted is the <u>difference</u> in temperature between his two horns. Since the horns are some 4 hours apart, the Milky Way appears first in the eastern horn (point B), then moves over to the western horn (point A). We can also see another portion of the Milky Way going from 3 to 8 hours.

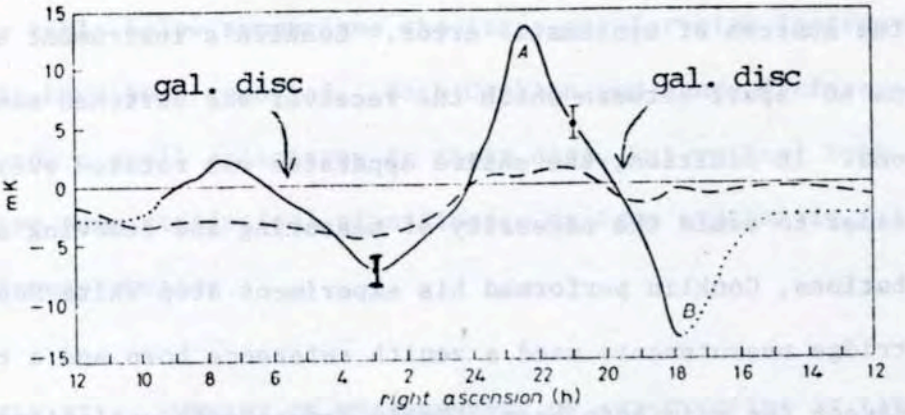

Fig. 6. – Mean of twenty-three observations; the data have been averaged over 1 h of right ascension. The dotted line indicates estimated values; the broken line shows the observations after subtraction of nonthermal contributions. Zero level is arbitrary; the total length of error bars is two standard deviations.

The solid line represents his measurement of the anisotropy. After extrapolating the measurements of the galactic background, and subtracting the extrapolated values from his data, he is left with the dashed line. Note that his measured anisotropy is dominated by galactic signal.

If his residual (the dashed curve) were due solely to the motion of the earth through the radiation, it would be a pure cosine function. Since it isn't, Conklin derives the amplitude and phase of the first Fourier component, and attributes these to the motion of the earth. We feel that his conclusion (that he is seeing the Aether Drift) is unwarranted, it is just as plausible that he is observing no more than the residual of an improper extrapolation.

Henry's experiment was limited by balloon flight operations to a single night's data-taking, and covered from 3-15 hours, in right ascension. Because of an oversight in the design of his instrument (his Dicke switch was sensitive to its orientation with respect to the earth's magnetic field) he was able to analyze only the north-south component of the mapping of the sky made by his instrument. The figure below shows the data after

the subtraction of the calculated galactic background. Typically, the north-pointed antenna saw 3.3 ± 1.2 x 10^{-3} °K cooler temperature than the south-pointed one. Using Conklin's curves to estimate the background removal, and taking into account the fact that at Henry's frequencies the galactic emission is reduced by approximately half, we find that Henry must have removed only about 3 x 10^{-3} °K from his data, and that only during the hour or two when his southern horn had the galactic disc in view. This would have been about 11 p.m. in the graph below. In fact, he reports that different assumptions about galactic background removal made only a 10 or 20% change in his measured result.

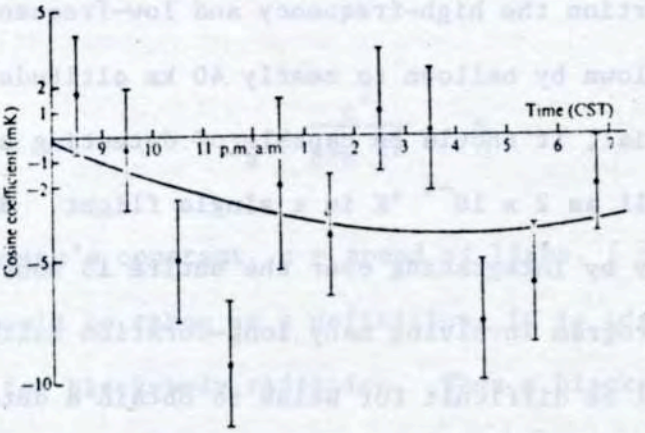

Fig. 7 Hourly averages of cosine coefficients corrected for galactic radiation. The curve is the best fit to a 24 h anisotropy. Error bars represent single standard deviation error limits.

The appearance of Henry's data suggests that he may have underestimated his errors by a factor of perhaps 1.5. Henry's stated value for the χ^2 of his data points to the fitted line, 18 for 9 degrees of freedom, gives a confidence level for his fit of only 2%. If he were to increase his error estimate to give a reasonable confidence level, his measured anisotropy would drop well below the two standard deviation level due to statistics, and we could not attach significance to his result.

We must conclude that the Aether Drift has not yet been observed. Conklin did a fine experiment, but was limited by galactic emission. We interpret his results to mean that no anisotropy has been observed to a sensitivity of $2 - 3 \times 10^{-3}$ °K. To push the sensitivity down to 2×10^{-4} °K, and see the anisotropy that must be there, one must operate at higher frequencies as planned in our experiment.

The group of R. Weiss at M.I.T. has an ongoing experiment to measure the anisotropy of the 3°K radiation. The experiment uses a twin-horn radiometer sensitive to two wavelength bands: 0.4 to 1 mm and 1 to 3 mm. Residual anisotropy caused by atmospheric background is reduced by combining in proper proportion the high-frequency and low-frequency measurements. The instrument is flown by balloon to nearly 40 km altitude and, if it achieves its full potential, it should be capable of detecting sky temperature differences as small as 2×10^{-4} °K in a single flight. Because this sensitivity is achieved only by integrating over the entire 13 hours of a balloon flight, and because a program involving many long-duration balloon flights is very arduous, it will be difficult for Weiss to obtain a detailed sky temperature map and separate the possible causes of an observed anisotropy at the 2×10^{-4} °K level. Nevertheless, the Weiss experiment is the first to have the capability of detecting the motion of the earth about the sun, and a preliminary flight has already matched the accuracy of Partridge and Wilkinson. Additional flights are planned for the near future.

C. Background and Noise -- detailed discussion

Looking for a small anisotropy in the 3 °K cosmic black-body radiation involves searching for an effect that is deeply buried in noise. We begin our discussion with a definition of "antenna temperature". We then discuss the sources which contribute noise to our detector, starting with the furthest away (galactic emission), and working our way in (stars, sun, planets, the atmosphere) until we get to the sources of noise in the detector itself.

1. Antenna Temperature

Let S be the power per unit bandwidth per unit area received by an antenna from a source. Define the "antenna temperature" T_a of that source to be

$$T_a = \frac{c^2}{8\pi k f^2} \cdot S$$

where k = Boltzmann's constant, c = speed of light, f = frequency. Although this formula should be taken as a definition, it is identical to the Rayleigh-Jeans equation for black-body radiation. Thus a black-body source filling the angular acceptance of the antenna will generate an antenna temperature equal to its black-body temperature, provided that the Rayleigh-Jeans formula is good in that frequency range. The power per unit bandwidth of a black body is given by the Planck formula:

$$S = \frac{(8\pi/c^2)\ hf^3}{e^{(hf/kT)}-1} \qquad h = \text{Planck's constant}$$

We therefore can calculate the antenna temperature of a black body with the interesting result that it is not constant with frequency:

$$T_a \text{ (black body)} = \frac{(hf/kT)}{e^{hf/kT}-1}\ T$$

This formula explains why the signal due to Aether Drift (figure on page 11) decreased with frequency when plotted in terms of antenna temperature. Antenna temperature is a useful term, and in the discussions that follow we shall use it to describe the various noises.

2. Galactic Background

The galactic background of microwave radiation is perhaps the most severe restriction on this experiment. At low frequencies the galactic background is the dominant anisotropy and does not fall below the tenths of a millidegree level except for frequencies greater than 30 GHz. At the tenths of a millidegree level it is possible to subtract galactic background out of the remaining signal, but only to an accuracy comparable to the galactic background itself. At 33 GHz the uncertainty in this subtraction will be about 0.16 millidegrees K. This value was deduced by extrapolating galactic radio maps at frequencies below one gigahertz. Note that this extrapolation is in agreement with the raw anisotropy observed by Conklin (page 25).

Galactic background was discussed on pages 8 - 10. This radiation is believed to arise from the synchrotron emission of energetic electrons. The observed energy distribution of cosmic ray electrons obeys the formula

$$\frac{dN}{dE} = c_1 E^{-n} \qquad \text{with } n = 2.6$$

c_1 = a constant

It can be shown that synchrotron emission from such a steeply falling spectrum should obey the following approximate formula:

$$S = c_2 f^{(1-n)/2}$$

$$= c_3 f^{-0.8} \qquad (\text{with } n = 2.6)$$

where S is the power per unit bandwidth and f is the frequency. The observed experimental distribution of spectral indices is shown below, and peaks between 0.7 and 0.8:

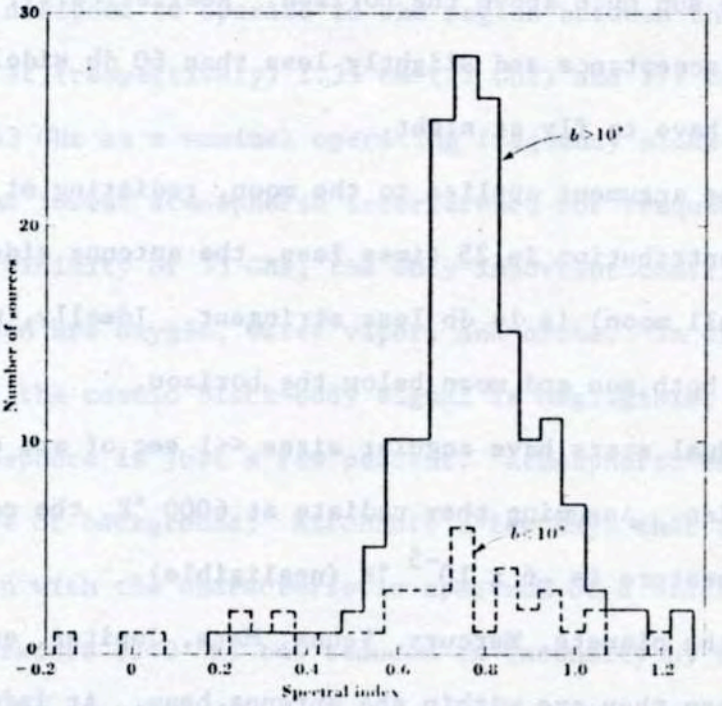

Figure 8. Number of nonthermal sources as a function of spectral index for galactic latitudes above 10° (solid curve) and below 10° (dashed curve). Taken from Kellermann, Ap. J. 140, 969 (1964)

When we translate S to antenna temperature, we pick up two powers of frequency to get the formula for synchrotron emission $T_a = f^{-2.8}$. The uncertainty in the spectral index is reflected in the width in the above plot.

3. The Sun, Moon, Stars, and Planets

Radiating at 6000 °K, the sun (solid angular size ~7×10^{-5} steradian) contributes 17 °K referred to an antenna with a 10° beamwidth. The antenna and shield system we expect to design will have 60 db sidelobe power reduction at 60°. In terms of temperature this would be ~17×10^{-6} °K or 2×10^{-5} °K with the sun on the horizon, an acceptable amount of noise - but unacceptable with the sun much above the horizon. Realistically, the antenna will have greater acceptance and slightly less than 60 db sidelobe rejection so that we will have to fly at night.

The same argument applies to the moon, radiating at 230 °K. Since this noise contribution is 25 times less, the antenna sidelobe rejection criterion (full moon) is 14 db less stringent. Ideally, we will be happy to operate with both sun and moon below the horizon.

Individual stars have angular sizes <<1 sec of arc or solid angle << 10^{-10} steradian. Assuming they radiate at 6000 °K, the contribution to antenna temperature is ~6×10^{-5} °K (negligible).

Among the planets, Mercury, Venus, Mars, Jupiter, and Saturn may be detectable when they are within the antenna beam. At inferior conjunction Venus has an apparent diameter of 67 sec of arc and a black body temperature of about 600° (J. Kraus, Radio Astronomy, McGraw-Hill, 1966). For a 10° beamwidth antenna of 3×10^{-2} steradian acceptance, T_a (Venus) = 1.7×10^{-3} °K. The other planets give lesser contributions, e.g. Jupiter, the next brightest, gives an average of about 10^{-4} °K.

These numbers suggest a possible calibration of our radiometer -- we should easily detect the presence of Venus in the acceptance of an antenna, but Jupiter only with great difficulty.

4. Atmospheric Emission

Although the galactic background decreases with increasing frequency, the atmospheric and electronic noise of the detector increase significantly with increasing frequency. These factors require that we choose as low a frequency as possible but above 30 GHz. Thus we plan to do our experiment in the K_A frequency band of communication using radar equipment which is specifically designed to operate in the region between the water vapor and oxygen lines at (respectively) 1.35 cm (22 GHz) and 1/2 cm (60 GHz). We have chosen 33 GHz as a nominal operating frequency since the region around 33 GHz has the lowest atmospheric interference for frequencies above 30 GHz.

In the vicinity of 33 GHz, the only important contributors to atmospheric emission are oxygen, water vapor, and ozone. In this frequency range absorption of the cosmic black-body signal is negligible, since the opacity τ of the atmosphere is just a few percent. Atmospheric emission is, however, a major source of background: Kirchhoff's law says that the atmosphere will emit radiation with the characteristic spectrum of a black body at its ambient temperature (240 °K) but reduced in intensity by the factor τ. Thus, for example, a τ of 0.026 (about sea level at 33 GHz) would result in emission yielding an antenna temperature of 6.4 °K.

Because of this we would like to get above as much atmosphere as we can. Vehicles for this purpose are listed in Table IV.

TABLE IV: ATMOSPHERE AND VEHICLES

Vehicle	Oxygen (Relative Pressure)	Water Vapor (Amount of Precipitable Water/unit Area)
Sea Level	1	0.7 ± 0.3 cm
Mountain Top (White Mt)	0.6	0.1 (9 mos.), 0.2 (June, July, Aug)
C-141 Observatory	0.15	few μm
U-2	0.06	negligible
Balloon	0.01	negligible
Satellite	0	0

The satellite would be the best vehicle and we feel strongly that this experiment will eventually be done from a satellite. But the satellite experiment will be expensive, and will have a long lead time; it is important to do the best possible experiment from an airborne platform in preparation for the satellite design. A balloon experiment has fewer difficulties with atmospheric emission than an airplane experiment, but is severely limited in the amount of sky that can be surveyed, due to the limited flight time, and risk of damage to the instrument. Because the atmospheric emission background <u>can</u> be handled successfully from an airplane platform, and because the airplane offers the advantages of (1) control of flight plan, (2) ability to repeat flight often (3) low risk to instrument, we have selected the airplane as the most appropriate vehicle for this measurement.

The amount of absorption (and re-emission) due to a given emission line is determined by the frequency of the line, its strength, and effective width. The line width is dominated by the effect of molecular collisions (pressure broadening). In this case the emission is well described by a summation of Lorentzian (Breit-Wigner) functions of the form

$$\frac{P}{(f-f_o)^2 + P^2}$$

where P is the line width, proportional to the pressure. For frequencies on the "tails" of resonances (such as the frequency we have chosen, 33 GHz) the observed emission will be proportional to the pressure.

The oxygen emission lines (at sea level) are shown in the following figure:

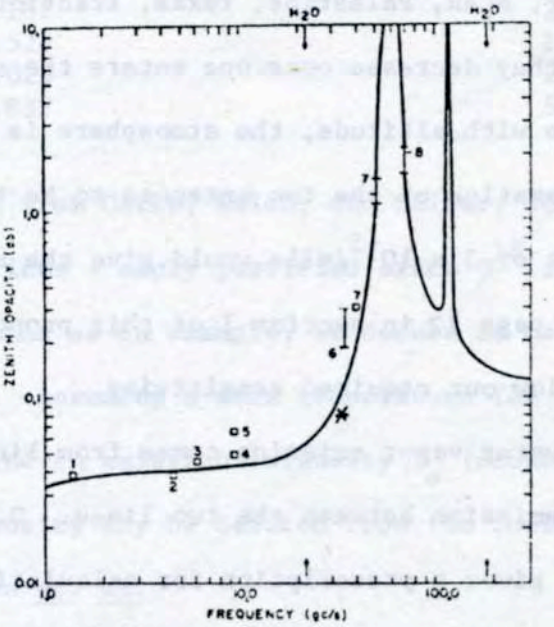

Figure 9. Oxygen emission at sea level from 1 to 200 GHz (taken from Meeks and Lilly, J Geophys. Res. 68, 1983 (1963)

At 33 GHz (indicated by the star) the zenith opacity is approximately 0.11 db, giving τ = .026, and an antenna temperature T = 6.4 °K. At 65,000 ft. the integrated amount of oxygen would be only 6% of that at sea level, bringing the antenna temperature down to 0.4 °K. The reduced width of the pressure broadened line should reduce T even further. If equal amounts of oxygen appeared above our two antennas, the total effect would be to raise the noise level of the receiver by about 0.4 °K, a negligible amount.

However, oxygen pressure gradients do exist, as can be seen on any weather map, and therefore the signals received by the two antennas may be different. We have estimated the typical pressure gradients that exist by studying weather maps (typical fractional gradients of $\frac{1}{P}\frac{dP}{dx} = 2 \times 10^{-5}$/mile), and tables of systematic North-South pressure gradients (Allen, Astrophysical Quantities, 1964, pg. 116 shows an average gradient of 10^{-5}/mile). According to W. Landsberger, NCAR, Palestine, Texas, fractional gradients at 45,000 ft are comparable; they decrease once one enters the stratosphere (where, because T increases with altitude, the atmosphere is stable). If we take the average beam separation of the two antennas to be ten miles, then a fractional pressure gradient of 3×10^{-5}/mile would give the anisotropic emission shown in the figure on page 12 in section I of this proposal, which is about a factor of two below our required sensitivity.

The major water vapor emission comes from lines at 22 GHz and 180 GHz, and a continuum emission between the two lines. D. Burch (J. Opt. Soc. Am. 58, 1383 (1968)) gives a prescription for calculating the intensity of these lines for the atmosphere. At 33 GHz, the opacity is 0.01 per gm/cm^2 of water. Assuming a temperature of 240 °K, this yields an emission temperature of 0.24 °K per mm precipitable water. (The terminology "mm precipitable" is used to indicate that the "mm" does not refer to "mm Hg", i.e. it is the amount of water, not the pressure of the water.) At 45,000 ft. the residual water vapor is only 2-3 μ prec. (P. Kuhn, M. Lojko, F. Peterson, Nature 223, 462 (1969)). Hence the average anisotropy for an hour of integration to yield a temperature difference of 2×10^{-4} °K would have to be 30-40%. At the mountain top altitudes, where the amount of water vapor is more than 100 times greater, small anisotropies in the water vapor are the most serious systematic source of error.

The atmosphere contains a layer of ozone between 20 and 40 altitude which absorbs the lethal part of the ultraviolet radiation from the sun; this layer also absorbs microwaves. The relevant ozone lines with their peak absorption intensities against the sun (6000 °K) are

f (GHz)	T rel. to sun (°K)
30.052	3.7
30.181	2.1
30.525	1.1
36.025	2.7
37.832	5.7

This list was taken from Caton, Welch, and Silver, JGR 72, 6137 (1967) and includes only O^{16} lines - amply justified since O^{18} is only 0.2% as abundant. Taking the 36 GHz line as an example, we deduce an ozone opacity of 2.7°/ 6000° = 4.5×10^{-4}. Assuming a mean temperature for the ozone of 240 °K (atmospheric) we find an emission intensity T_a (ozone) = .11 °K at the peak. At 33 GHz, the intensity may be deduced from the following formula, given in the article by Caton et. al:

$$\Delta f = 52.7 \frac{P\ (mm)}{T} \quad MHz$$

and the Breit-Wigner formula given above. Above U-2 altitude, the average ozone altitude (30Km) corresponds to a pressure P ≈ 9 mm. Thus. Δf = 30 MHz - we are 100 half-widths away and T_a is entirely negligible. The same conclusion follows for the other lines and thus we can forget about ozone; - even if it were extremely irregularly distributed. Note, however, that we have chosen our frequency (33 GHz) to be well away from all emission lines. If for some reason we decide to change our frequency we must reconsider the effects of ozone.

5. Receiver noise and Environmental noise

Noise introduced by the detector falls into several categories: thermal noise, absolute calibration drift, asymmetry between components, orientation sensitivity and environmental sensitivity.

Receiver thermal noise is random, and can be removed by integration over a long period of time. In effect, we are averaging together many measurements. If the bandwidth of the detector is B, then its coherence time is $t_c = 1/B$. For an integration time t we get effectively n independent measurements, where $n = t/t_c$. Since the signal will be coherent (in constant phase with the detecting signal) for the entire detection time, but the noise will be coherent only over the time t_c, the signal-to-noise ratio will improve as the square-root of n:

$$\frac{dT}{T} = \frac{1}{\sqrt{n}} = \frac{1}{\sqrt{t/t_c}} = \frac{1}{\sqrt{t\ B}}$$

where T is the noise temperature of the apparatus, and dT is the 1 standard deviation sensitivity of the detector. A precise derivation leads to and formula $dT/T = k/\sqrt{tB}$, where k is a numerical constant (typically between 1 and 2) that depends on the detailed design of the apparatus.

All components of the detector introduce thermal noise in proportion to their insertion loss (i.e. their absorptivity). The most serious of these is the first amplifier in the system. The components before the amplifier - the antenna, waveguides and so forth are made of copper or similar metals and have a very low emissivity (10^{-3}). Their contributions to the antenna temperature scale down from their ambient temperatures by their emissivity. The components after the amplifier are less important by the factor of the amplifier gain (probably a factor ~30). The noise figures for various off-the-shelf components are given in section IID.

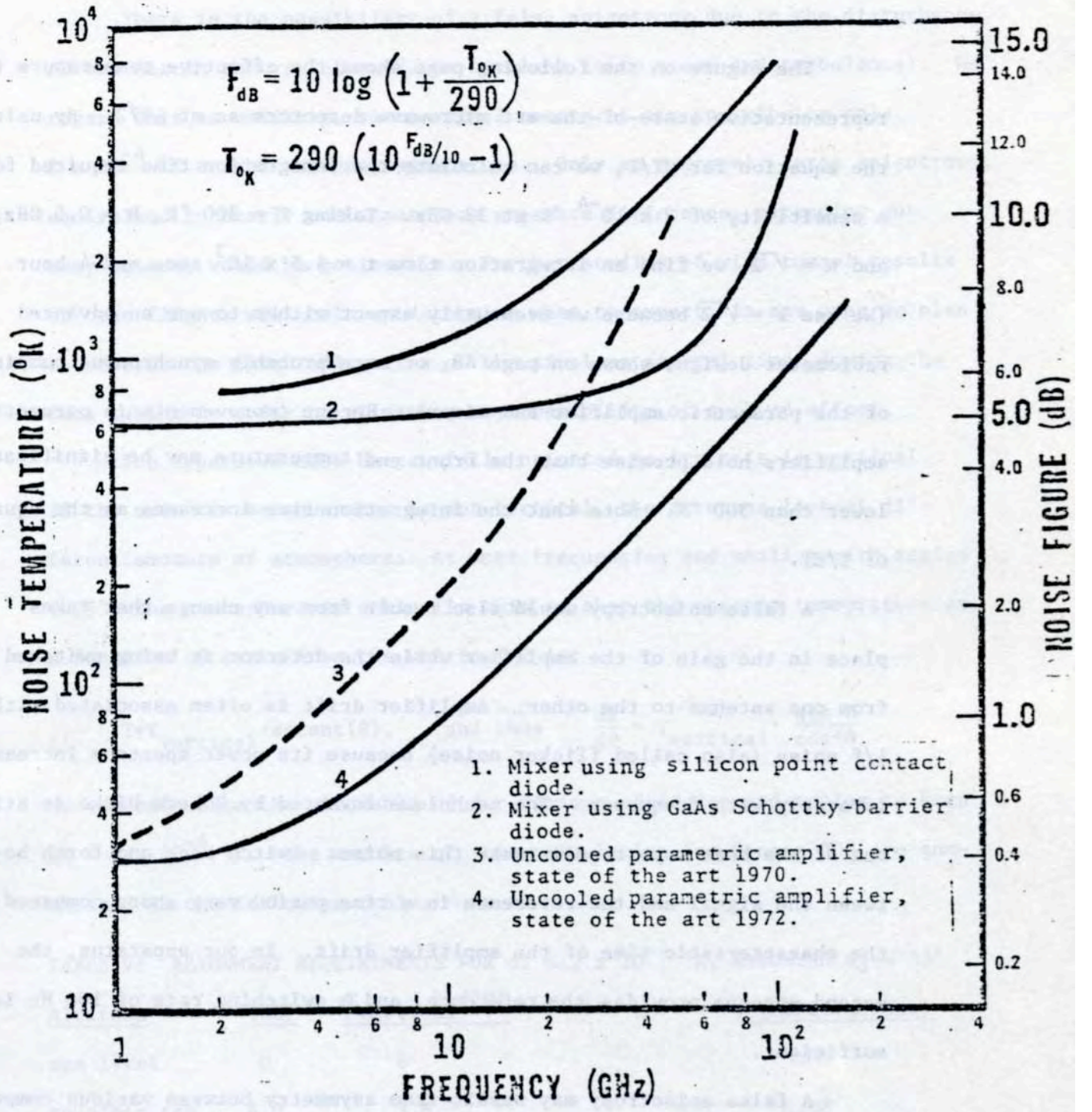

Figure 10: Effective noise temperature and noise figure as functions of frequency for microwave receiver with mixer diodes and parametric preamplifier inputs.

The figure on the following page shows the effective temperature for representative state-of-the-art microwave detectors as of 1972. By using the equation for dT/T, we can calculate the integration time required for a sensitivity of 2×10^{-4} °K at 33 GHz. Taking T = 300 °K, B = 0.5 GHz, and $k = \sqrt{2}$, we find an integration time $t = 4.5 \times 10^{3}$ sec. = 2.4 hour. (We use $k = \sqrt{2}$ because we eventually expect either to use an advanced radiometer design, shown on page 48, or more probably synchronous pumping of the parametric amplifier and mixer). Recent improvements in parametric amplifiers hold promise that the front end temperature mav be significantly lower than 300 °K. Note that the integration time increases as the square of T/dT.

A false anisotropy would also result from any change that takes place in the gain of the amplifier while the detector is being switched from one antenna to the other. Amplifier drift is often associated with 1/f noise (also called flicker noise) because its power spectrum increases inversely with frequency. The technique invented by Robert Dicke is still one of the best ways to eliminate this noise: switch back and forth between the signal and the reference in a time period very short compared to the characteristic time of the amplifier drift. In our apparatus, the second antenna provides the reference, and a switching rate of 100 Hz is sufficient.

A false anisotropy may result from asymmetry between various components, especially the two antennas. The antennas must be matched as carefully as possible, and small additional sources of noise should be added if necessary to achieve this balance. During operation the horns will be physically interchanged at periodic intervals (once per minute) in order to average out any small residual asymmetries.

There is the possibility of a false anisotropy due to the disturbance of the air in the vicinity of the airplane (slip steam and turbulence). We regard this as unlikely, since each 3 meters of air contributes only 1×10^{-4} °K to the antenna temperature. Only an extremely large anisotropy, equivalent to nearly one atmosphere pressure difference, extending out many meters, would be noticeable. Further studies of wind tunnel results or test flights will help us determine what to expect; in any case we plan to reverse the flight direction of the airplane several times during the data taking in order to eliminate the possibility of such an effect.

The apparatus must be carefully oriented so its axis is vertical. If the axis of the apparatus is not vertical, the antennas look at different amounts of atmosphere. At most frequencies and small zenith angles (<75°) the atmosphere is optically thin so that the antenna temperature as a function of angle from the vertical θ is:

$$T = T_{vertical} \cdot \text{secant}(\theta), \quad \text{and thus} \quad \frac{dT}{d\theta} = T_{vertical} \cdot \frac{\sin\theta}{\cos^2\theta}$$

We can calculate the allowable $d\theta$ for various altitudes and angles to keep $dT < 2 \times 10^{-4}$ °K. The results of this calculation for θ near 30° are summarized in the following table.

TABLE V: ALIGNMENT REQUIREMENTS FOR $dT < 2 \times 10^{-4}$ °K, ASSUMING $\theta_o = 30°$

Altitude	(km)	$T_{vertical}$ (°K)	$d\theta$ (milliradians)
sea level	0	6	0.05
mountain top	4.0	3.6	0.08
45 k feet	13.7	0.94	0.3
65 k feet	20	0.4	0.75
100 k feet	30.0	0.073	4.0
very high	-	0	-

The U-2 has a roll stability of about 4.5 milliradians/second with a period of 2 to 5 seconds. A typical roll angle is about 3 milliradians; about four times worse than the total average we would like to achieve. Unless the U-2 has a large systematic list or very irregular behavior, we expect that simply bolting the apparatus into the U-2 and adjusting it to be level while still on the ground will be quite adequate. By monitoring the angle to local vertical, we can be sure to average out the atmospheric background (perhaps we will have to make a small correction to the data or to adjust the apparatus on a simple orientation platform). One such simple orientation platform would maintain an average local vertical through adjustments whose time constant was long compared to the natural frequency of the U-2. Although the rms angular variation may be significant the total average angle from vertical can be as small as we require.

At the U-2 altitude nearly all atmospheric background is due to oxygen since the water vapor is lower or frozen out. Therefore, a good monitor of local vertical is the oxygen emission itself. We would like to monitor the oxygen at the frequency where it is the dominant signal but is not so strong as to be saturated. The greatest sensitivity ($dT/d\theta$) occurs at the frequency where the overlying atmosphere optical depth d(f) is about unity, i.e. $d(f) \simeq \frac{t_v}{\tau(f)} \frac{1}{\cos\theta} \simeq 1$; where t_v is the vertical thickness, $\tau(f)$ is the mean attenuation length at frequency f and $\theta = 30°$ is the angle from vertical (for 65,000 feet $t_v \simeq 62$ gm/cm^2). We can then scale the sea level zenith opacity from Figure 9 on page 34 [by $62/1020 * 1/\cos(30°) = 0.07$] to find d(f) in db (multiply by $\frac{\ln 10}{10} = 0.23$ to find zenith opacity in standard units). At sea level the optimal frequency for oxygen monitoring is ~50 GHz where $d(f) \simeq 1$. At the U-2 altitude we would like to monitor the oxygen in the range 55-60 GHz which, unfortunately, is near

the peaks of the oxygen lines instead of on their wings. We may find it necessary to move down to a frequency slightly below the oxygen lines in order to simplify the interpretation of the oxygen monitor results. The amount of oxygen emission at 33 GHz relative to that at the oxygen monitor frequency will differ with altitude because of pressure broadening. Using the sea-level peak-to-wing ratio of about 200 to 1, we find we need to integrate the oxygen monitor for approximately 6 seconds for our desired orientation accuracy if we utilize a 1000 °K mixer-receiver with a single side bandwidth of 0.4 GHz. Taking into account the reduced pressure at U-2 altitude we note that the peak-to-wing ratio increases significantly reducing the needed integration time to less than about 1 sec.

Other orientation asymmetries are somewhat less difficult to handle than the angle to local vertical. For example, the effect of the earth's magnetic field on the electromagnetic switches and other microwave components can be minimized by magnetic shielding. Likewise the apparatus may be sensitive to mechanical stress. Care must be taken in its design to make the apparatus free from such stresses as occur when the antennas are interchanged.

D. Instrumentation and Flight Vehicle

We describe here in detail the instrumentation required to achieve the signal-to-noise levels discussed in the preceeding sections. A schematic diagram showing the major features of the apparatus as they will fit into the U-2 is shown in the figure on the next page.

For the purpose of this discussion we have divided the detector system into four subsystems. We want to emphasize that this division is artificial. Many of the design criteria, the final configuration, and many of the design parameters of one subsystem are integrally related to those of the others.

In section 1 we discuss the 33 GHz radiometer and the data recording system. We present a block diagram for the receiver, and emphasize that it can be built with off-the-shelf components. In section 2 we discuss the antenna system which will be necessary to meet our sidelobe rejection requirements. Section 3 describes the mechanical support and system for precise orientation of the radiometer and antennas. Finally in section 4 we discuss the specifications of the U-2 and of the alternative flight vehicles we considered.

FIGURE 12

CROSS-SECTIONAL VIEW OF THE U-2 WITH RADIOMETER INSTALLED

(UNITS ARE INCHES)

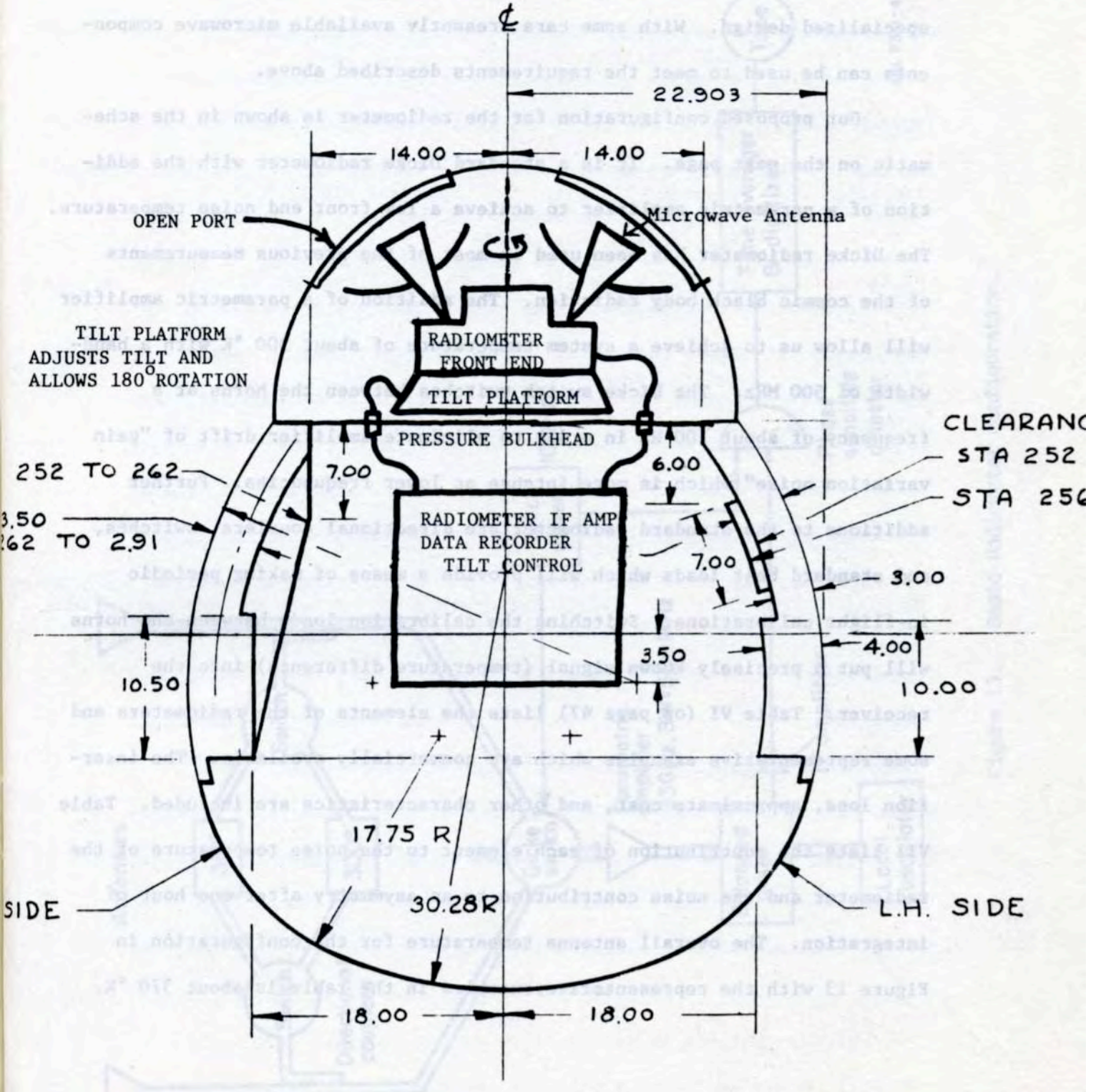

VIEW LOOKING AFT

1. The Radiometer and Data Recording System

We describe here the details of the receiver -- the details of the antenna design are left to the following section. In general the receiver and data recording system will require no development and very little specialized design. With some care presently available microwave components can be used to meet the requirements described above.

Our proposed configuration for the radiometer is shown in the schematic on the next page. It is a standard Dicke radiometer with the addition of a parametric amplifier to achieve a low front end noise temperature. The Dicke radiometer has been used in most of the previous measurements of the cosmic black body radiation. The addition of a parametric amplifier will allow us to achieve a system temperature of about 300 °K with a bandwidth of 500 MHz. The Dicke switch switches between the horns at a frequency of about 100 Hz in order to eliminate amplifier drift of "gain variation noise" which is more intense at lower frequencies. Further additions to the standard radiometer are directional couplers, switches, and standard heat loads which will provide a means of making periodic in-flight calibrations. Switching the calibration loads between the horns will put a precisely known signal (temperature difference) into the receiver. Table VI (on page 47) lists the elements of the radiometers and some representative examples which are commercially available. The insertion loss, approximate cost, and other characteristics are included. Table VII lists the contribution of each element to the noise temperature of the radiometer and the noise contribution to an asymmetry after one hour of integration. The overall antenna temperature for the configuration in Figure 13 with the representative examples in the table is about 370 °K.

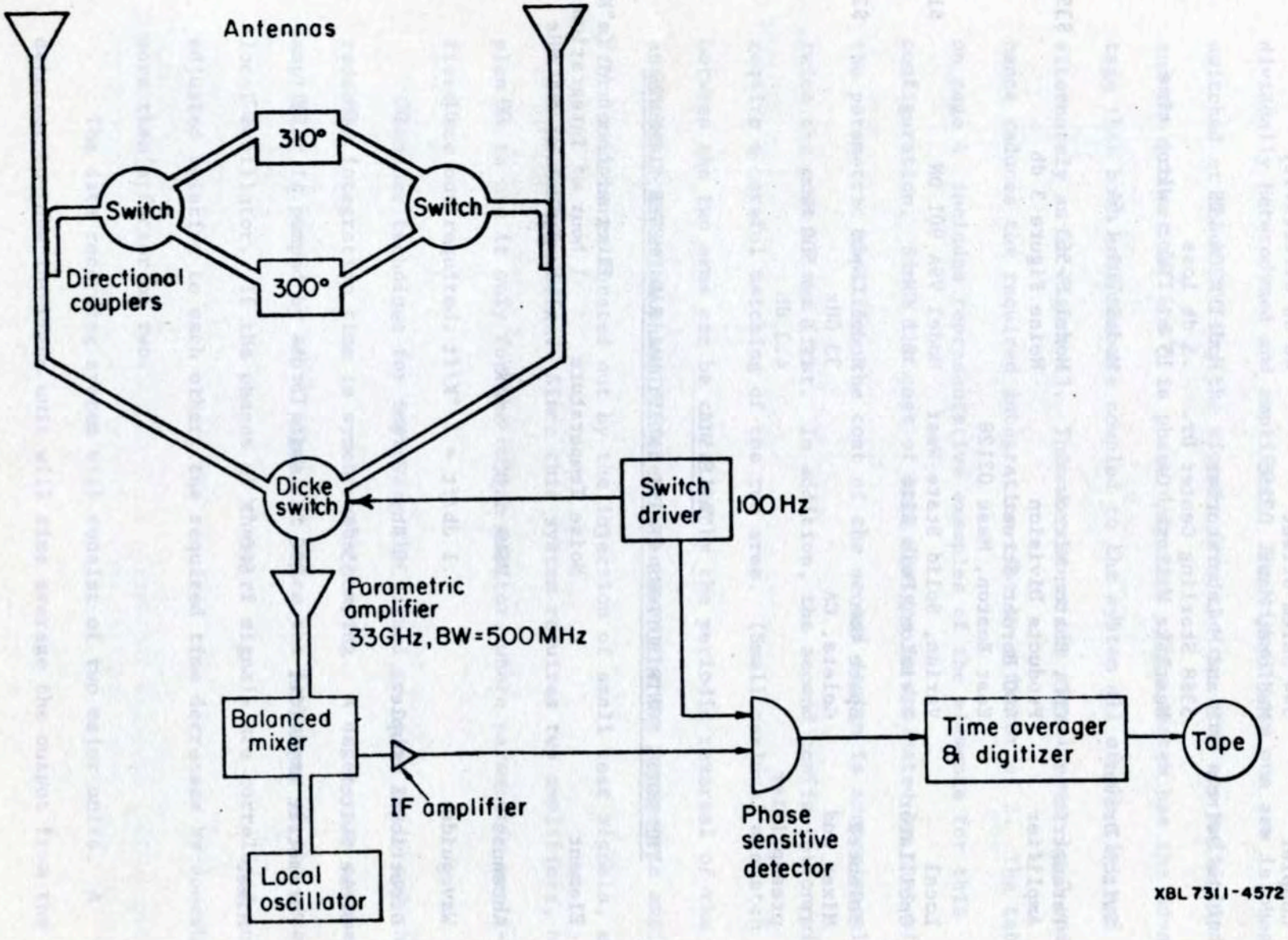

Figure 13. Basic Radiometer configuration.

TABLE VI: REPRESENTATIVE EXAMPLES OF ELEMENTS OF THE RADIOMETER

Element	Manufacturer	Characteristics	Cost
Directional Coupler	Baytron 344 Salem Street Medford, Mass. 02155	30 db 40 db directivity	$250
Dicke Switch	E and M Laboratories 5388 Sterling Center Dr. Westlake Village, CA	Model R204 LTS .5 db loss 15 millisec switch time	$750
Switch Driver	"	Model EDS 1.5A	$525
Parametric Amplifier	CDC, Boston Microwave Products Division 400 Border Street East Boston, Mass 02128	Model S-563 Noise Figure 3 db	$35,000
Local Oscillator	Varian, Solid State West Division, Palo Alto	Model VSA 901 DN 32.5 GHz	$1,210
Balanced Mixer and IF preamplifier	Space Com Goleta, CA	Model CK-13 33 GHz IF 5 to 500 MHz 4.3 db	$2,300

TABLE VII

THE NOISE CONTRIBUTIONS OF THE INDIVIDUAL RADIOMETER ELEMENTS

Element	Noise Temperature	Fluctuation of ΔT (m°K) after 1 hour of integration with a bandwidth of 500 MHz
Antennas	VSWR 1.05: < 4°K	.00
Waveguide	.1 db/ft = 7 °K/ft	.01
Directional couplers	30 db; .3 °K	.00
Dicke Switch	55 °K	.04
Parametric amplifier	290 °K, Gain 15 db	.22
Mixer	600 °K	.02

A more advanced configuration (suggested by Prof. J. Welch) is shown in Figure 14. Here the signals from the two antennas (A and B) are mixed in a magic T and the resulting sum (A + B) and difference (A - B) are individually heterodyned and amplified. The signal from one arm is phase switched at about 100 Hz, the signals from the two arms are multiplied, and the product $(A^2 - B^2)$ is phase detected. This system has the advantage that both antennas are coupled to the system all of the time and not alternately as in Figure 13. This increases the signal power by 2 and hence reduces the required integration time by a factor of 2. The table on page 4 includes representative examples of the elements for this configuration. Since the cost of both designs is dominated by that of the parametric amplifier the cost of the second design is approximately twice the cost of the first. In addition, the second configuration will require a careful matching of the two arms. (Small residual mismatch between the two arms can be cancelled by the periodic reversal of the antennas). Relative phase differences between the two parametric amplifiers will be calibrated out by the injection of small test signals, as in the preceding design. Since this system requires two amplifiers, our plan is to use it only for the oxygen monitor, where parametric amplifiers are not required.

Another technique for improving the signal to noise ratio and thus reducing integration time is synchronous pumping. A degenerate parametric amplifier is pumped by an rf signal at twice the frequency of the mixer local oscillator. If the phases of these rf signals are correlated and adjusted relative to each other, the required time decreases by somewhat more than a factor of two.

The data recording system will consist of two major units. A detector-to-tape interface unit will time average the output from the

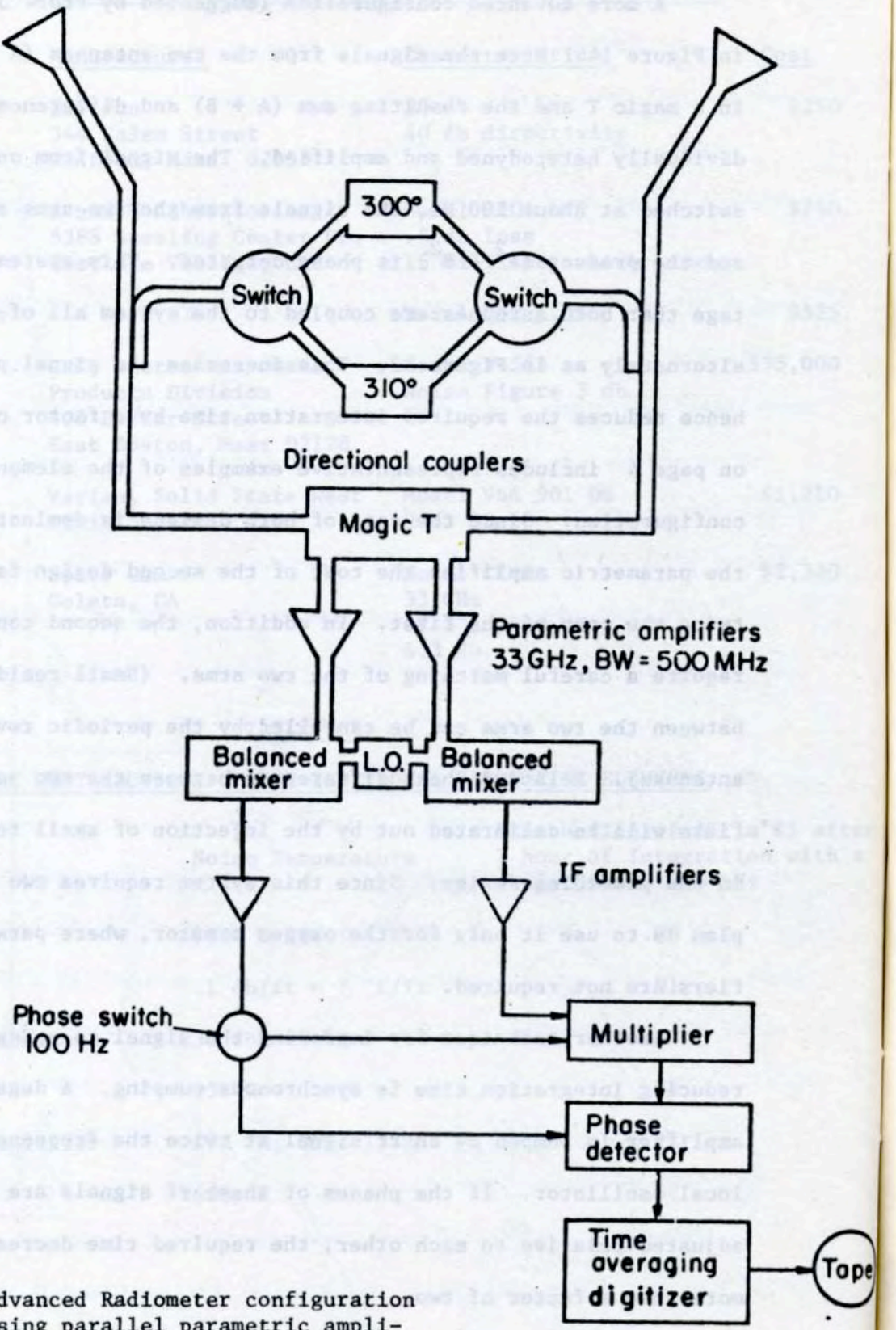

Figure 14: Advanced Radiometer configuration using parallel parametric amplifiers to increase detected power by a factor of two.

phase sensitive detector over a period of about 10 seconds. It will digitize this average as well as a variety of environmental parameters (temperature, pressure time, etc.) and antenna orientation. The data will be written on tape for later analysis. The second major unit will be a sequencing unit which controls the averaging time, the periodic switching of the antennas, and the periodic calibration switching. The data acquisition rate will be low (about 12 bytes/minute) thus no tape changing will be necessary during the flight. It is anticipated that the experiment will be completely automatic. The power requirement of the detector and recording system will be about 200 watts.

2. Antenna-Shield System

There are three major considerations in the antenna design: the beam width, reflections by the antenna of the receiver noise back into the receiver, and the backlobe and sidelobe rejection.

The beamwidth required for the experiment is not tightly defined by the experimental goals. A stationary beam will sweep out 15 degrees in the sky in a typical one hour averaging time; we would gain little resolution by making our beamwidth substantially narrower than 15 degrees. The beamwidth is limited on the upper end by considerations of its acceptance of radiation from sources other than the sky. These will be discussed below.

The reflections of the receiver noise back into the receiver is characterized by the voltage standing wave ratio, VSWR. The power reflection co-efficient is given by $\rho = ((1-VSWR)/(1+VSWR))^2$. For a standard open horn antenna a VSWR of 1.05 or better is typical. For either system described in the previous section, this would contribute about 0.2 °K to the antenna temperature. Almost all previous experiments measuring

the cosmic black body radiation have used open horns. The possibility exists of using lenses within the horns to shape the radiation pattern. These lenses can be readily matched with quarter wave layers or simulated quarter-wave layers to achieve a VSWR of 1.05.

A rough and extremely conservative estimate of the sidelobe and backlobe (integrated) rejection needed can be obtained by assuming one horn sees the earth (300°K) to some extent and the other horn doesn't. In order to reduce this 300 °K asymmetry to 0.3 m°K requires a 60 db rejection of the earth's radiation. The easiest way to achieve this rejection is to erect large reflecting screens around the antennas so that most of the natural sidelobe pattern of the horns is looking symmetrically at the relatively cold sky. With these screens the only radiation accepted from the earth is that which diffracts around the edge of the screen. By arranging the edge of the screens to be near a minimum of the horn radiation pattern, diffraction can be reduced further. Almost all of the previous measurements of the cosmic blackbody radiation have used screens to suppress the earth's radiation. It may be possible to install such a ground plane shield on the U-2. It might consist of a conductor several inches wide, (possibly covered with an insulating layer), extending out from the sides of the upper hatch in a zero-lift geometry.

Another approach to the sidelobe problem is simply to use an antenna design that achieves the required sidelobe suppression. The figure below shows the measured radiation pattern for an antenna built by Bell Laboratories; the pattern agrees with that predicted from theory, and meets our requirements. Scaled down to operate at 9 mm, this antenna design would be a tight squeeze in the upper hatch of the U-2. We will probably use a combined design of low sidelobe antenna, with some type of ground plane

shield. Fortunately, there is a considerable technology available at Lockheed on the design and behavior of antennas specifically for the U-2 aircraft.

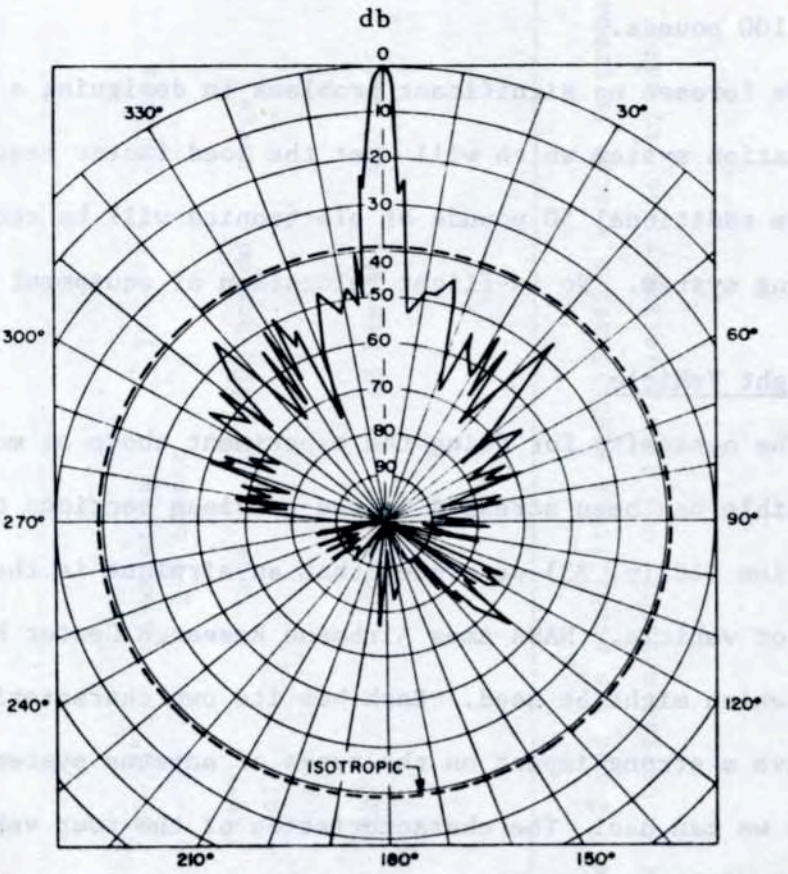

An overall radiation pattern of a horn reflector measured by the short-pulse method at 3.74 kMc; transverse plane, longitudinal polarization.

(from Advances in Microwaves, L. Young, Vol. 3, Academic Press, 1968).

We have also considered other antenna designs. We have consulted with a number of people in the country who are working on advanced antenna design or have operated antennas where side lobe rejection was a problem. We have been assured by them that either a reactive wall horn or a dual mode horn could be designed to meet our requirements. One particular manufacturer* with considerable experience in building antennas can produce a reactive wall horn with a radiation pattern down by about 50 db at 60° off axis. An improved design including shields would satisfy our requirements.

---

* Ancom Inc., Milpitas, Calif.

3. Mechanical Support

The antennas will be interchanged (rotated 180°) approximately every minute. The combined weight of the antennas and receiver will be between 50 and 100 pounds.

We foresee no significant problems in designing a mechanical support and rotation system which will meet the load factor requirements of the U-2. An additional 50 pounds of electronics will be required for the data recording system. No in-flight relocation of equipment will be necessary.

4. Flight Vehicle

The necessity for doing the experiment above as much of the atmosphere as possible has been stressed in the previous sections on atmospheric noise. In section IIC (p. 33) we argued that an airplane is the most attractive choice of vehicle. NASA Ames Airborne Research Center has a number of planes which might be used. Each has its own characteristics and these will have a strong impact on the types of antenna system and stabilization systems we can use. The characteristics of the four vehicles considered so far are summarized in Table VIII.

The U-2 has several features which make it the most attractive vehicle. Because of the high attainable altitude, water vapor emission is negligible. Oxygen emission is reduced to the level where the U-2 autopilot stabilization is probably all that is required. The U-2 has the advantage that the instrument bay is symmetrically located in the aircraft, so that the antennas will look out from the aircraft symmetrically. A photograph of the U-2 is reproduced on page 54.

TABLE VIII: CHARACTERISTICS OF AIRPLANES UNDER CONSIDERATION

Airplane	Cruising Altitude	Time at Cruising Altitude	Windows Size	Windows Elevation	Stabilized Platform	Maximum Flight Frequency	Payload Limits	Electrical Power
U-2	65,000 ft	6.5 hr	28"x54"	bay	none *	100 hrs/mo.	460 lbs	320-450 Hz, 208/120V 8KVS; 28 V D.C., 100 Amps; 400 Hz, 115 V, 750 VA
Lockheed C-141A	45,000 ft	3.5 hr	36" dia.	35-75°	existing ± 6 arcsec	?	400 lbs	
CV-990	40,000 ft	2.0 hr	12"x14" 12"x14"	65° 90°	none	100 hrs/mo.	large	400 Hz, 200/115V, 40 KVA 60 Hz, 115V, 14KVA
Model 23 Lear Jet	45,000 ft	1.9 hr	14" dia	22°	none	48 hrs/mo.	400 lbs	400 Hz, 115 V, 6.5 amps; 60 Hz, 115 V 9.5 amps; 28 V D.C., 30 amps.

* Because of the high altitude attained by the U-2 and its stability, a stabilization system is probably not necessary; however, a simple platform (using an oxygen monitor) would be relatively easy to add.

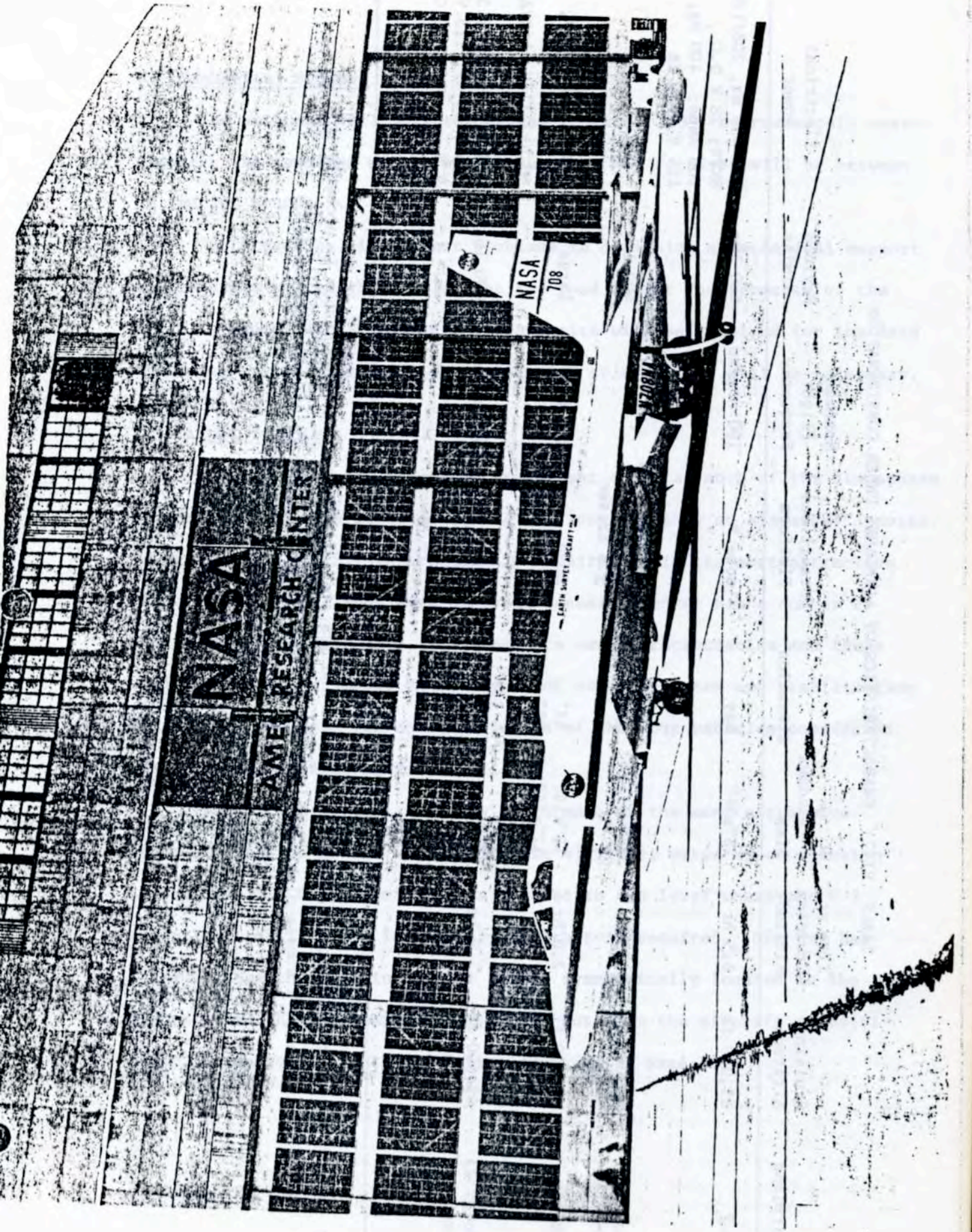
NASA
AMES RESEARCH CENTER
NASA
708
EARTH SURVEY AIRCRAFT

III. EXPERIMENTAL PROGRAM

The complete experimental program will require two years. About nine months of the first year will be devoted to the design, fabrication and testing of all instrumentation, and the installation of the detector into the aircraft. During the final quarter of the year the package will be flight tested and a number of data collection flights will be made. Significant new physics will be derived from these initial flights. The second year will be devoted to a systematic mapping of the northern sky at 33 GHz. Little additional instrumentation will be required for the second year; the dominant effort will be data collection and computer analysis.

a. First Year Program (July 1974 to July 1975)

We have divided the experimental program for the first year into three main phases:

i. System Design

ii. Subsystem Fabrication, System Integration, and Check Out

iii. Data Collection and Analysis

The important features of each phase are shown on the flow chart on the next page. In the three sections that follow we describe the goals and activities of each phase.

1. System Design

In Section II above we describe the requirements for the experiment to achieve a sufficient signal-to-noise to map the sky at 33 GHz. We have emphasized the interdependence of the elements of the instrumentation and the program and have stressed the impact that the design of one element has on the others. We will complete the detailed design of the instrumentation and formulate a detailed observing program during an initial two-month phase.

TWO YEAR PROGRAM FOR AETHER DRIFT EXPERIMENT

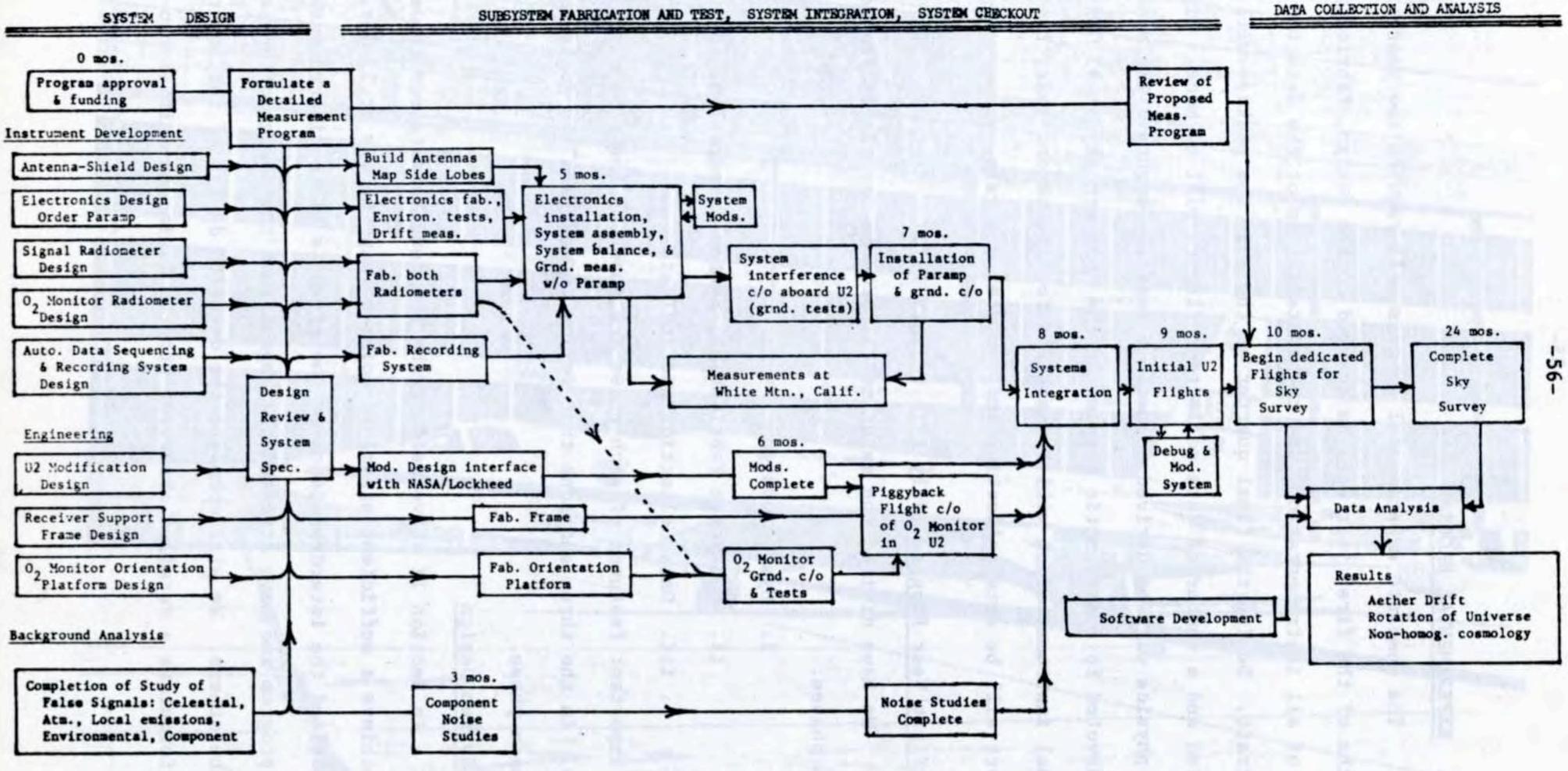

We will specify the modifications required on the U-2, and negotiate them with Lockheed Inc. The required modifications are expected to be relatively minor, and consist primarily of creating windows in the upper hatch. Such windows will be designed to be compatible with future astronomical experiments. During this time we will also make a detailed design of the radiometer and data recording system, design the antenna-shield system, design the oxygen monitor and rotation platform, continue our analysis of backgrounds, and order those elements which have a long acquisition time. This phase will end with a complete design review. (See flow chart.)

The mechanical subsystems involve the largest number of interfaces between various components. The antenna-shield system, the receiver support frame, the orientation platform, and the aircraft must all be compatibly combined. Since modifications to the airplane will require about four months the specification of these modifications will be made as soon as possible. The design of the airplane interfaces and modifications will be carried out in cooperation with the people at NASA Ames and Lockheed Corporation.

The antenna design involves the development of antennas and shields with excellent rejection of radiation from the earth and airplane. This development presently involves building a prototype system and measuring its radiation pattern. The design of the antenna-shield system will depend strongly on the final airplane environment. The addition of a ground-plane shield to the aircraft would greatly reduce the cost and complexity of the antenna system.

The design of the radiometer and data recording system is not strongly coupled to the other aspects of the instrumentation. As discussed above, the fabrication and noise analysis of these systems is well understood. The microwave technology for this frequency region is well developed and high

quality commerical components are readily available. The major item for the radiometer is the parametric amplifier which has an acquisition lead time of about six months.

At the end of the design stage we will carry out a design review in which the total experiment package will be scrutinized for compatability and effectiveness. This review will include a reconsideration of the major branch decisions involving specification of the airplane modifications, choice of the stabilization technique, antenna-shield design, electronics design, structural layout, and the requirements of the data collection flight program.

2. Subsystem Fabrication System Integration and Check Out

After the design review we will begin construction of the various subsystems. We expect to buy and borrow the individual components and do most of the fabrication ourselves. The major exception is the parametric amplifier which will be commercially built to our specifications.

With the exception of the parametric amplifier the elements required for the signal radiometer and the oxygen monitor radiometer can be purchased within 60 days. The calibration and matching of these elements and the assembly and testing of the radiometers will take place as soon as the elements are available. With some initial support from Lawrence Berkeley Laboratory we have borrowed or purchased many of the elements for the signal radiometer. By the fall of 1974 we would like to have both radiometers assembled and to test their sensitivity at mountain altitudes (White Mountain, California). Laboratory tests will be made to test their sensitivity to thermal shocks and vibrations. The parametric amplifier will be integrated into the signal radiometer when it is received.

Concurrent to the assembly and testing of the radiometers we will build an automatic data sequencing and recording system. This system will provide timing and logic for interchanging the antennas, making time averages, and digitizing and recording the averaged signals. In addition it will periodically record the temperature and pressure of the radiometer environment.

As the assembly of the radiometers is completed the construction effort will be placed on the fabrication of the orientation platform capable of responding to the oxygen monitor, and the frame to support and rotate the radiometers and acoustically isolate them from the aircraft.

During subsystem testing we will make a complete mapping of the radiation pattern of the antennas. Using a pulsed testing procedure we hope to measure the pattern down to 60 db.

As the individual subsystems are completed and tested they can be integrated into the final detector. The end of this integration phase will see the detector installed in the airplane. Testing and check out of some of the subsystems can be done piggyback during daylight hours, when the U-2 is being used for earth survey studies. Several flights will be required to insure full compatability and reliable operation of the complete system.

During this integration phase initial work will begin on developing software for the final data analysis.

3. Data Collection Program and Analysis

Important astrophysics will be derived from the first few flights. A significant anisotropy due to the "Aether Drift" will probably be observable after just the first few hours of integration. Of course, a number of flights is necessary to show that the source of the anisotropy is cosmic and to explore its nature. The scheduling of the overall data collection program

will depend on the final configuration of the detector and the availability of the airplane. These data collection flights will require night time dedicated missions.

b. Second Year Program

Ideally, we would like to map the temperature of the entire sky. With the detector described in Section II we need an integration time of slightly over two hours to achieve a sensitivity of 2×10^{-4} °K. This means a complete northern sky survey would require 4π steradian hours. If we resolve the sky into 15° (0.26 radian) bins it will thus require about 200 hours to map the northern sky. No new instrumentation will be required for the second year's program. In addition to the extensive flight program, the major effort on the experiment will be the computer data analysis.

IV. Estimated Costs

During the first half of fiscal year 1975, we expect work on the production of the experimental hardware and refining experimental concepts. We do not expect to begin systematic accumulation of data until calendar year 1975.

We show here (Table IX) a rough and somewhat unorthodox breakdown of estimated costs for this program. A more detailed breakdown follows (Table X).

Hopefully, this breakdown enables one to determine the major remaining cost area of the program. The salaries include one full time research assistant (graduate student) and 1/2 FTE of the approximate 2 FTE Ph.D. physicists working on the project. Most of these personnel are shared with superconducting magnetic spectrometer cosmic ray balloon group (NASA Grant NGR05-003-553) or other groups at the University of California, Berkeley. Thus even though one individual may be specified in these categories he does not necessarily work full time throughout the program but is shared. This sharing allows us a larger reservoir of ability to draw on.

TABLE IX

Budget Summary

	Fiscal 1975 (Thousands of Dollars)	Fiscal 1976
Personnel Costs	18.1	26.3
Supplies & Expense	3.0	3.0
Travel	4.0	4.0
Overhead for above	5.3	7.0
	30.5	40.3
Equipment & Apparatus	49.0 (35.0 for parametric amplifier)	6.0
TOTAL	79.5	46.3

Detailed Aether Drift Experiment Budget for Fiscal Year 1975

				Amount Requested
I.	Salaries & Wages	Monthly Rate	Percent of Time	
	No. Classification			
	1 Asst. Res. Physicist III	1357	50%	8,142*
	1 Graduate Student Research Assistant	741	50%-9 mos 100%-3 mos	5,558
				13,700
II.	Employee Benefits			
	15% of salary marked *			1,221
III.	LBL Facilities Usage			
	21.6% of $15,070 (salaries + 10%)			3,255
			TOTAL PERSONNEL COSTS	18,176
IV.	Supplies and Expense			
	A. Travel (See page 65 for breakdown)	4,000		
	B. LBL General Services shops, stores, maintenance	2,000		
	C. SSL technical reports, communications, typing, editing, drafting	1,000		
			SUPPLIES AND EXPENSE	7,000
V.	Equipment			
	A. Parametric Amplifier	35,000		
	B. Microwave horn antenna	4,000		
	C. Components (waveguides, attenuators, hybrid tees, etc.)	3,000		
	D. Oxygen monitoring system components	7,000		
			EQUIPMENT	49,000
VI.	Total Direct Costs			74,176
VII.	Indirect Costs 21.2% of $25,176 (MTDC)			5,337
VIII.	TOTAL AMOUNT REQUESTED FY 1975			$79,513

IX. University Contribution

Clerical assistance within the Space Sciences Laboratory (including University overhead and employee benefits). $2,459

X. Lawrence Berkeley Laboratory Contribution

Lawrence Berkeley Laboratory will pay 25% of the salaries of R. Muller, T. Mast, G. Smoot, A. Buffington, and C. Orth for work on this proposal. LBL will also make available mechanical and electrical engineering and technician services up to 1/2 FTE. Based on current salary, indirect costs and employee benefits this represents an additional contribution of about $44,000. Based on the total experiment costs of $126,000, the LBL contribution is 35%.

IV. A. Detail	Cost
A. Trips to Vendors	
1. Boston Microwave - CDC	500
(parametric amp) or Westinghouse, Baltimore	
2. Antenna Design Inco, L.A.	400
B. Field Operations	
1. White Mountain - several trips	700
2. Moffett Field, etc.	400
C. Conference & Discussions	
1. Washington D.C. 2 people	1000
2. New York 2 people	1000
	$4000.

Estimated Budget for FY 1976

				Amount Requested
I.	**Salaries & Wages**			
	No. Classification	Monthly Rate	Percent of Time	
	1 Asst. Res. Physicist III	1425	50%	8,550 *
	1 Graduate Student Research Ass't	778	50%-9 mos 100%-3 mos	5,835
	1 Sr. Programmer-Technician	1324	33%	5,291 †
			PERSONNEL COSTS	19,676
II.	Employee Benefits			
	15% of salary marked *			1,283
	12% of salary marked †			635
				1,918
III.	LBL Facilities Usage			
	21.6% of $21,594 (salaries + 10%)			4,675
			TOTAL PERSONNEL COSTS	26,269
IV.	Supplies and Expense			
	A. Travel	4,000		
	B. Misc.	3,000		
			SUPPLIES AND EXPENSE	7,000
V.	Equipment			
	Modifications, Alterations, Replacements			6,000
VI.	Total Direct Costs			39,269
VII.	Indirect Costs (21.2% of $33,269)			7,053
VIII.	TOTAL AMOUNT REQUESTED FY 1976			$46,322
IX.	University of California Contribution			$1,432
X.	Lawrence Berkeley Laboratory Contribution.		(We expect the L.B.L. contribution to remain constant)	

PERSONNEL

From the cost breakdown given in the preceding section, one sees that this experiment will employ two full-time-equivalent (FTE) physicists, and one graduate student. The FTE's will come from our astrophysics group, which consists of five physicists. It is expected that two of the physicists will devote a major fraction of their time to this experiment, and the rest of their time to the other research activities of the group. Prof. Luis Alvarez expects to devote 25% of his time to this research project. The other physicists will work on this experiment at about the 25% level. The other activities of our group include an effort to determine the age of cosmic-ray nuclei through balloon-borne measurement of the isotopic abundance of Be^{10} and completion of the data analysis for previous balloon experiments.